European Journal of Medicinal Chemistry xxx (xxxx) xxx

Contents lists available at ScienceDirect

European Journal of Medicinal Chemistry

journal homepage: http://www.elsevier.com/locate/ejmech

Design, synthesis and biological evaluation of novel thiosemicarbazone-indole derivatives targeting prostate cancer cells

Zhang-Xu He [1], Jin-Ling Huo [1], Yun-Peng Gong, Qi An, Xin Zhang, Hui Qiao, Fei-Fei Yang, Xin-Hui Zhang, Le-Min Jiao, Hong-Min Liu[**,2], Li-Ying Ma[***,2], Wen Zhao[*,2]

State Key Laboratory of Esophageal Cancer Prevention and Treatment, Key Laboratory of Advanced Pharmaceutical Technology, Ministry of Education of China, School of Pharmaceutical Sciences, Zhengzhou University, Zhengzhou, Henan, 450001, PR China

ARTICLE INFO

Article history:
Received 25 June 2020
Received in revised form
21 October 2020
Accepted 25 October 2020
Available online xxx

Keywords:
Prostate cancer
Thiosemicarbazone
Proliferation
Cell cycle
Apoptosis

ABSTRACT

To discover novel anticancer agents with potent and low toxicity, we designed and synthesized a range of new thiosemicarbazone-indole analogues based on lead compound **4** we reported previously. Most compounds displayed moderate to high anticancer activities against five tested tumor cells (PC3, EC109, DU-145, MGC803, MCF-7). Specifically, the represented compound **16f** possessed strong antiproliferative potency and high selectivity toward PC3 cells with the IC_{50} value of 0.054 μM, compared with normal WPMY-1 cells with the IC_{50} value of 19.470 μM. Preliminary mechanism research indicated that compound **16f** could significantly suppress prostate cancer cells (PC3, DU-145) growth and colony formation in a dose-dependent manner. Besides, derivative **16f** induced G1/S cycle arrest and apoptosis, which may be related to ROS accumulation due to the activation of MAPK signaling pathway. Furthermore, molecule **16f** could effectively inhibit tumor growth through a xenograft model bearing PC3 cells and had no evident toxicity *in vivo*. Overall, based on the biological activity evaluation, analogue **16f** can be viewed as a potential lead compound for further development of novel anti-prostate cancer drug.

1. Introduction

Development of potent anticancer agents with low toxicity and high selectivity are urgently necessary for tumor treatment [1–3]. Metal chelation is a promising strategy in developing chemotherapy drugs due to the elevated requirement of cancer cells for critical metals (Fe, Cu, and Zn) needed in growth and proliferation [4–6]. Several metal chelators (Fig. 1), including NNS, ONS, NNN, ONN or hydroxamic acid donor chelators, displayed potent antiproliferative potency [4,6–13]. In particular, thiosemicarbazones (TSC) derivatives featuring the NNS donor revealed extensive and long-term pharmacological effects [14–19], especially antitumor activity [20–22]. Anticancer activity of TSCs was connected with the perturbation of intracellular metal homeostasis, the formation of redox active complexes, which resulted in the generation of reactive oxygen species (ROS) [5,23–27], or the effect on several crucial proteins, such as ribonucleotide reductase, PARP-1, MEK and EGFR [28–31]. In addition, several TSC-chelators targeting DNA synthesis [27,32,33] and cell-cycle inhibition [23,34,35] also revealed potentially antiproliferative activity. Considering the key role of TSCs in cancer treatment, several novel thiosemicarbazone ligands had been identified and investigated in clinical trials, including 3-AP, DPC and COTI-2 (Fig. 1) [10]. Although this series of agents were generally explored, the side effects had partly limited their clinical utility [8]. Thus, the development of novel TSCs with potent and less toxicity were urgently needed.

Our group had previously reported that compound **1** (Fig. 2) was a potent anticancer agent toward MGC803 cells with the IC_{50} value of 4.01 μM and significantly suppressed cancer cell migration and invasion *in vivo* and *in vitro*, of which the TSC moiety attached to pyrimidine skeleton brought about our interest due to its potential anticancer activity [36]. Thus, a series of phenyl-substituted TSC derivatives (**series 1**) were synthesized, and most of them exhibited strong biological activity against MGC803 cells, more active in comparison to compound **1**, but moderate selectivity between MGC803 and normal cells [37,38]. Given improved cytotoxicity

* Corresponding authors.
** Corresponding author.
*** Corresponding author.
E-mail addresses: liuhm@zzu.edu.cn (H.-M. Liu), maliying@zzu.edu.cn (L.-Y. Ma), zhaowen100@139.com (W. Zhao).
[1] Both authors contribute equally to this work.
[2] These senior authors contribute equally to this work.

https://doi.org/10.1016/j.ejmech.2020.112970
0223-5234/

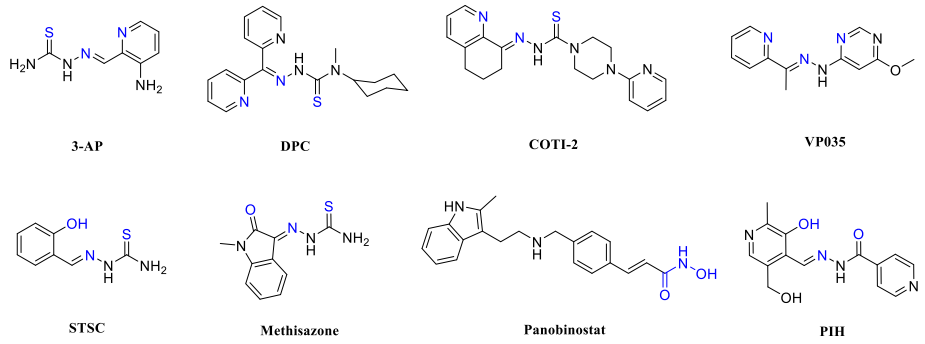

Fig. 1. Representative compounds with diverse chelate fragments. The donor atoms were highlighted with blue. (For interpretation of the references to color in this figure legend, the reader is referred to the Web version of this article.)

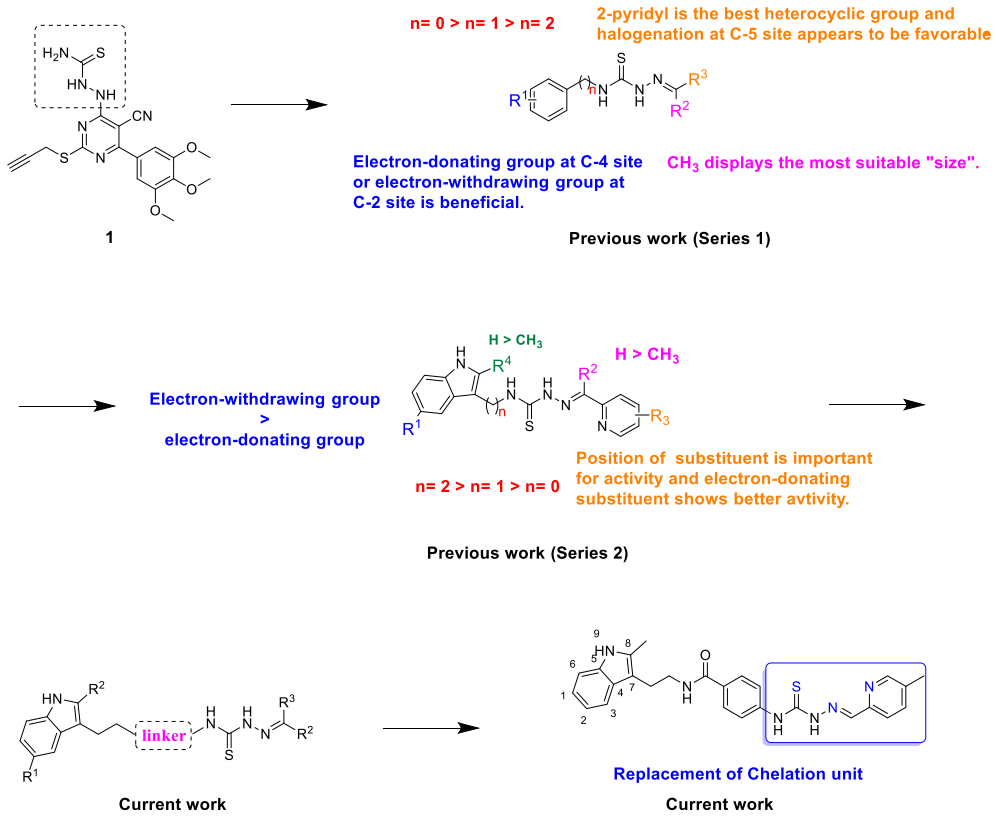

Fig. 2. Rationale for the design of novel thiosemicarbazone derivatives.

mentioned above, a series of TSC compounds (**series 2**) featuring various indole moieties were obtained and evaluated toward three cancer cell lines (MGC803, PC3, EC109). In contrast, compared with **series 1**, most analogues tethering the indole moiety showed more active against PC3 cells with the IC_{50} value of low micromolar range and higher selectivity. The preliminary structure-activity relationship (SAR) indicated that the number of carbon between indole and thiosemicarbazone might play an important role on potency [39]. We speculated that opportunities for optimization could be provided by changing various linker types. In current work, we firstly carried out systematic SAR study after exploring the effect of linker on antiproliferative activity. Also, several other donor chelators were combined with indole moiety, reported as a privileged motif [40], to exam potential inhibitory activity on cancer cells (Fig. 2). Herein, we designed and synthesized a novel series of TSC derivatives as potent anti-prostate cancer agents based on our previous work, and explored their potential mechanism.

2. Results and discussion

2.1. Chemistry

The overall synthetic routes of the title compounds were illustrated in Schemes 1–7. Compound **4** was efficiently synthesized from commercially available **1** following our previously reported methods (Scheme 1) [39]. The materials 2-(1H-indol-3-yl) ethan-1-amine **1** was firstly reacted with carbon disulfide in the presence of triethylamine, followed by the addition of DMAP and Boc_2O to give the

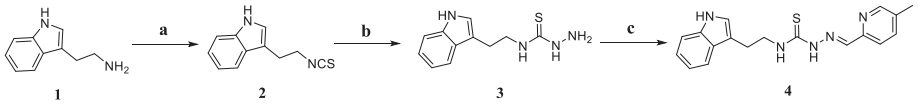

Scheme 1. Reagents and conditions: (a) (1) CS_2, TEA, EtOH, rt; (2) Boc_2O, DMAP, EtOH, rt; (b) hydrazine hydrate, DCM, rt; (c) 5-methylpicolinaldehyde, acetic acid, EtOH, rt.

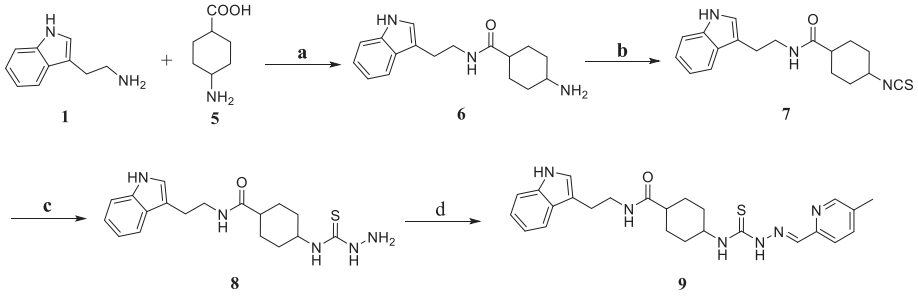

Scheme 2. Reagents and conditions: (a) EDCI, HOBT, DCM, rt; (b) (1) CS_2, TEA, EtOH, rt; (2) Boc_2O, DMAP, EtOH, rt; (c) hydrazine hydrate, DCM, rt; (d) 5-methylpyridine-2-carbaldehyde, acetic acid, EtOH, rt.

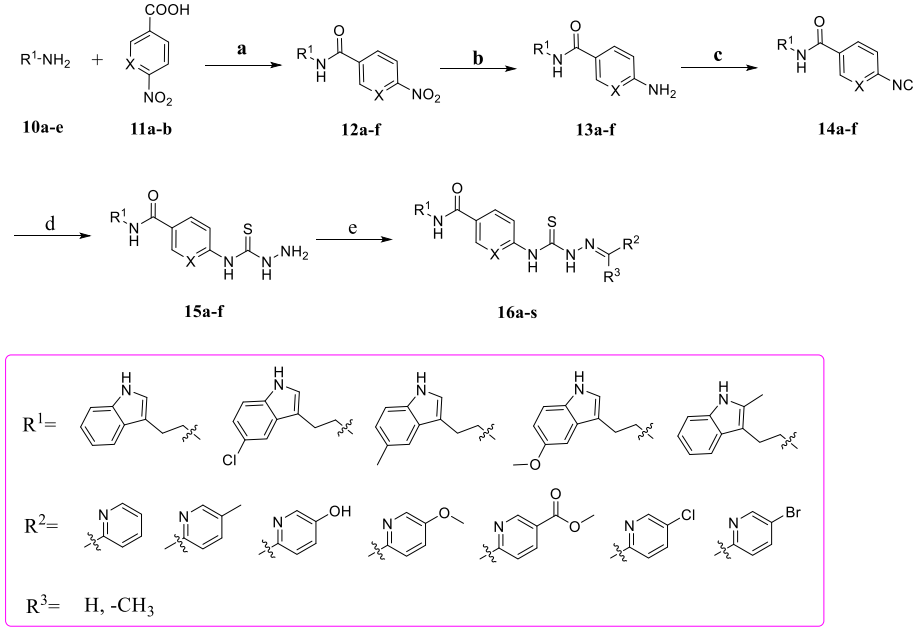

Scheme 3. Reagents and conditions: (a) EDCI, HOBT, DCM, rt; (b) H_2, Pt–C, MeOH, rt; (c) (1) CS_2, TEA, EtOH, rt; (2) Boc_2O, DMAP, EtOH, rt; (d) hydrazine hydrate, DCM, rt; (e) appropriate aldehyde or ketone, acetic acid, EtOH, rt.

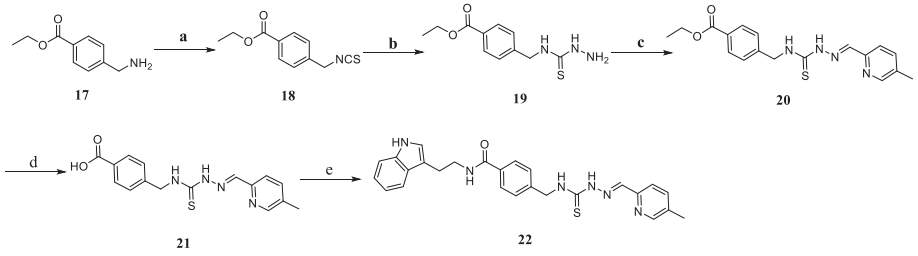

Scheme 4. Reagents and conditions: (a) (1) CS_2, TEA, EtOH, rt; (2) Boc_2O, DMAP, EtOH, rt; (b) hydrazine hydrate, DCM, rt; (c) 5-methylpyridine-2-carbaldehyde, acetic acid, EtOH, rt; (d) NaOH, H_2O, 80°C; (e) EDCI, HOBT, DCM, rt.

intermediate **2**, which was reacted with hydrazine hydrate to furnish compound **3**. Finally, compound **4** was afforded *via* the acid-catalyzed Schiff base condensation of **3** and 5-methylpicolinaldehyde in 69% yields. In Scheme 2, amide **6** was obtained from 4-aminocyclohexane-1-carboxylic acid **5** by reaction with EDCI, HOBT and raw material **1**, then provided TSC compound **9** according to our literature methods in

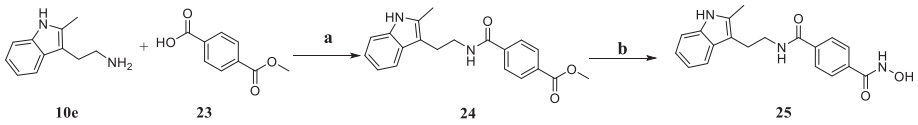

Scheme 5. Reagents and conditions: (a) EDCI, HOBT, DCM, rt; (b) NH_2OH, NaOH, THF/MeOH (1:1), 0 °C to rt.

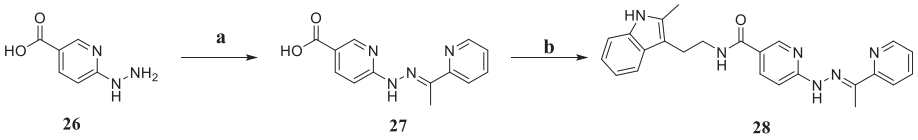

Scheme 6. Reagents and conditions: (a) 2-acetylpyridine, acetic acid, EtOH, 80 °C; (b) 2-(2-methyl-1H-indol-3-yl)ethan-1-amine, EDCI, HOBT, DCM, rt.

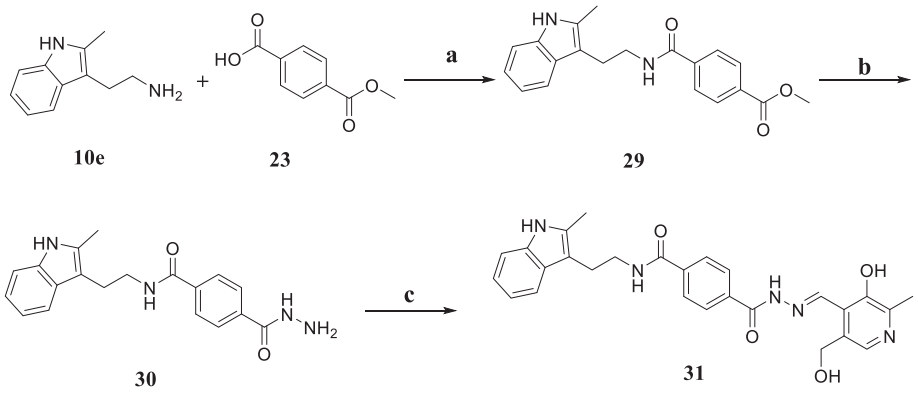

Scheme 7. Reagents and conditions: (a) EDCI, HOBT, DCM, rt; (b) hydrazine hydrate, MeOH, 80 °C; (c) pyridoxal hydrochloride, acetic acid, EtOH, 80 °C.

32% yields [39]. Intermediates **13a-f** were efficiently synthesized from the corresponding amines through two steps (Scheme 3). Specifically, substituted amines were reacted with 4-nitrobenzoic acid or 6-nitronicotinic acid in the presence of EDCI and HOBT in dichloromethane to yield **12a-f**, which was then reacted with H_2 in the presence of palladium to afford the corresponding **13a-f**. Intermediates **13a-f** were further converted to compounds **16a-s** through a similar reaction of Scheme 1a, b and c in 35–65% yields. In Scheme 4, intermediate **20** was also synthesized from raw material **17** as described for the synthesis of Scheme 1a, b and c. The hydrolysis reaction of compound **20** with sodium hydroxide resulted in compound **21** in 41% yields, which was further converted to the desired derivative **22** by condensation with 2-(1H-indol-3-yl) ethan-1-amine in 46% yields. Similarly, condensation of commercially available **10e** with 4-(methoxycarbonyl) benzoic acid **23** yielded **24** in 48% yield, which was further reacted with hydroxylamine in the presence of sodium hydroxide to afford compound **25** in 56% yields (Scheme 5) [41]. In Scheme 6, commercially available **26** was reacted with 2-acetylpyridine, in the presence of a catalytic amount of acetic acid (AcOH), *via* condensation reaction, leading to the formation of intermediate **27** in 53% yield, which was then transformed into compound **28** through under the catalysis of EDCI and HOBT in 50% yields. In Scheme 7, raw material **23** and **10e** were converted to the intermediate **29** using EDCI and HOBT in dichloromethane. The compound **29** was reacted with hydrazine hydrate to afford **30** in 65% yield. Finally, compound **31** was provided from a condensation reaction between **30** and pyridoxal hydrochloride in 41% yield.

2.2. Evaluation of biological activity

2.2.1. Antiproliferative activity

The *in vitro* anticancer activities of all synthesized analogues were examined against a panel of cell lines, including PC3 (human prostate cancer cells), EC109 (human esophageal cancer cells), DU-145 (human prostate cancer cells), MGC803 (human gastric cancer cells), MCF-7 (human breast cancer cells) and WPMY-1 (normal human prostate cells) by using the MTT assay [39]. **3-AP** and **DPC** were used as positive controls. Generally, the prostate cancer cells (PC3, DU-145) revealed more sensitive to most derivatives in comparison to other cancer cells. To investigate the importance of the linker that attached to indole and TSC moiety, we performed further modifications of the linker by introducing various amide groups into compound **4**. As shown in Table 1, compared with compound **4**, compound **9** with a cyclohexyl suggested weak inhibitory activity against PC3 cells. Surprisingly, conversion of the cyclohexyl in compound **9** into a phenyl group resulted in **16a**, which had an IC_{50} value of 0.241 μM in PC3 cells, about 2.5 times more potent than compound **4** ($IC_{50} = 0.601 \pm 0.042$ μM) with less toxicity against normal prostate cells WPMY-1. Besides, changing the linker from the phenyl to pyridyl afforded derivative **16b**, which showed comparable or decreased activity against five tested cancer cell lines as well as obvious toxicity in comparison to compound **16a**. Further, replacement of phenyl in **16a** with benzyl provided compound **22**, which was inferior to **16a** against PC3 and EC109 cells. These results indicated that the benzamide fragment as the linker was preferred.

Table 1
The anticancer activity of synthetic derivatives against the tested cell lines.

Comp.	structure	IC_{50} (μM)[a]					
		PC3	EC109	DU-145	MGC803	MCF-7	WPMY-1
4	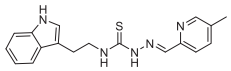	0.601 ± 0.042	4.512 ± 0.930	3.128 ± 0.210	5.655 ± 1.194	9.095 ± 0.96	2.328 ± 0.367
9	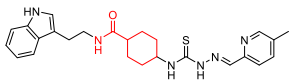	2.223 ± 0.345	14.120 ± 1.150	2.217 ± 0018	4.576 ± 0.660	8.129 ± 0.910	1.565 ± 0.195
16a	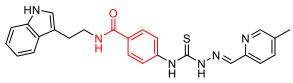	0.241 ± 0.050	3.938 ± 0.585	1.458 ± 0.156	7.015 ± 0.846	7.107 ± 0.852	12.476 ± 1.210
16b	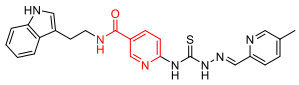	0.512 ± 0.120	12.515 ± 1.097	6.149 ± 0.312	7.590 ± 0.880	8.317 ± 0.920	2.501 ± 0.398
22	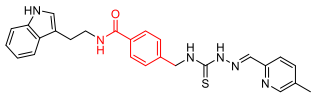	1.424 ± 0.153	18.500 ± 1.267	1.204 ± 0.258	4.847 ± 0.685	8.623 ± 0.936	1.093 ± 0.039

[a] Inhibitory activity was assayed by exposure various concentrations of the tested compounds for 72 h to substance and expressed as concentration required to inhibit tumor cell proliferation by 50% (IC_{50}). Data are presented as the means ± SDs. All experiments were carried out at least three independent times.

Next, compounds **16c-f** were synthesized to explore the effect of substituents in the indole group. As shown in Table 2, no matter an electron-withdrawing (-Cl) or -donating group (-CH_3, −OCH_3) substitution at indole 2-position, the title compounds **16c-e** displayed increased inhibitory activity toward PC3 cells as compared to no substitution compound **16a**, suggesting that substituent at indole 2-position was well tolerated. Among these, analogue **16e** revealed promising potency on PC3 with an IC_{50} of 0.061 μM, about 4 times more potent than **16a**. Surprisingly, introduction a methyl group into 8-position of the indole resulted in compound **16f** (IC_{50} = 0.054 ± 0.012 μM), which significantly improved potency on PC3 cells comparing to **16a** (IC_{50} = 0.241 ± 0.050 μM) with less toxicity toward normal prostate cell WPMY-1. These results showed that substituents on the indole ring were critical for antiproliferative activity.

With the improved potency and our better SAR understanding, we next focused on the effect of R^2 on activity. Our previous results indicated that the position of substituent in the pyridine ring was important for activity with a relative order of 4 > 2 > 3 > 5-position [39]. Thus, derivatives **16g-o** were synthesized to further explore the effect of the substituent in 4-position of pyridyl, and the results were shown in Table 2. Analogues (**16f**, **16l**) with electron-donating substituents displayed better potency than that of compound **16j** with no substituent. A similar trend was also observed (**16g** vs. **16e**, **16i**). The hydroxyl group was an exception to this trend and significantly decreased anticancer activity relative to its parental compound (**16g** vs. **16h**, **16j** vs. **16k**). In contrast, electron-withdrawing substituents (-Br, -Cl) at 4-position on the pyridine ring were detrimental to anticancer activity toward PC3 cells (**16j** vs. **16n**, **16o**). The above results suggested that electronic effect on the pyridine ring was important for potency. In addition, changing methoxy of compound **16l** into a larger ester group (**16m**) significantly decreased biological activity, suggesting that the increase of steric hindrance at 4-position of pyridine ring may be detrimental to target PC3 cells. Replacement hydrogen (**16j**) at the R^3 position with methyl (**16p**) was not conducive to improve activity toward five cancer cells. Similarly, derivatives **16g** and **16q** also exhibited this trend, and the compound **16q** with the IC_{50} of 0.947 μM was about 7 folds less potent than **16g** (IC_{50} = 0.133 ± 0.014 μM).

Several derivatives containing ONS, NNN, ONN and hydroxamic acid chelate fragments exhibited potential anticancer activity [4,6–11,42]. Thus, we replaced NNS with these donor chelators to further investigate antiproliferative activity and as was shown in Table 3. Replacement of NNS in compound **16f** with ONS fragment (**16r**, **16s**) led to obviously decreased potency, which may be attributed to their different ability to chelate iron [10]. In addition, when changing NNS to hydroxamic acid or ONN group (**25** or **31**) at compound **16f**, the activity was completely abrogated. Compound **28** containing the NNN donor showed moderate inhibitory activity toward five cancer cells; however, its toxicity against WPMY-1 cells stood out. These results indicated the NNS donor played a critical role on inhibiting cancer cells growth and reducing toxicity.

Generally, this series of TSC derivatives were more selective to prostate cancer cells over other cancer cells, which might be associated with multiple factors. Firstly, types of the linker were essential for selectivity. Particularly, introduction of benzamide group into compound **4** significantly increased selectivity (**4** vs. **16a**). Substituents in the indole ring and pyridine ring also affected the selectivity profile (**16a** vs. **16f**, **16f** vs. **16m**). Besides, compounds featuring an NNS fragment showed better selectivity than those with other chelate fragments (**16f** vs. **16s** or **28**). More importantly, in comparison to positive control 3-AP and DPC, most of the synthesized thiosemicarbazone derivatives exhibited comparable activities against PC3 cells, as well as lower toxicity toward normal WPMY-1 cells. Given markedly inhibitory activity and high selectivity in prostate cancer cells, we next explored the potential antitumor mechanism of compound **16f** using PC3 and DU-145 cells.

2.2.2. *Effect of compound **16f** on growth inhibition in human prostatic cancer cell lines PC3 and DU-145*

MTT assay was used to determine the cell viability for 24 h, 48 h and 72 h on PC3 and DU-145 cell lines, respectively. As shown in Fig. 3A, compound **16f** evidently inhibited the proliferation of PC3 and DU-145 cells in a dose- and time-dependent manner. Studies have revealed that iron chelators could form redox-active iron complexes, inducing cytotoxicity *via* Fenton chemistry [43]. To confirm whether these TSCs derivatives can act as iron chelators,

Table 2
The anticancer activity of derivatives **16a-q** against the tested cell lines.

Comp.	R^1	R^2	R^3	IC_{50} (μM)[a]					
				PC3	EC109	DU-145	MGC803	MCF-7	WPMY-1
16a	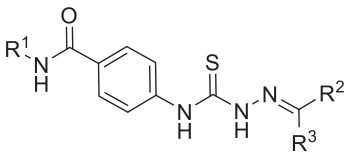		H	0.241 ± 0.050	3.938 ± 0.585	1.458 ± 0.156	7.015 ± 0.846	7.107 ± 0.852	12.476 ± 1.210
16c	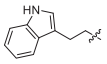		H	0.121 ± 0.032	2.399 ± 0.380	0.925 ± 0.031	2.671 ± 0.427	7.275 ± 0.862	7.092 ± 0.707
16d			H	0.081 ± 0.012	1.632 ± 0.213	1.064 ± 0.016	3.115 ± 0.493	4.017 ± 0.604	10.903 ± 0.950
16e	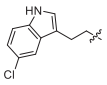		H	0.061 ± 0.020	5.746 ± 0.242	3.217 ± 0.159	10.424 ± 1.018	5.326 ± 0.706	18.095 ± 1.207
16f			H	0.054 ± 0.012	4.942 ± 0.694	1.439 ± 0.258	4.724 ± 0.674	5.334 ± 0.728	19.470 ± 1.242
16g	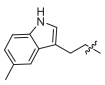		H	0.133 ± 0.014	5.027 ± 0.701	4.128 ± 0.294	5.346 ± 0.728	6.491 ± 0.812	12.251 ± 1.011
16h			H	2.485 ± 0.395	>20	15.248 ± 1.059	>20	>20	>20
16i	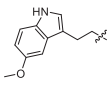		H	0.093 ± 0.053	9.116 ± 0.960	4.218 ± 0.176	8.924 ± 0.951	1.956 ± 0.291	>20
16j			H	0.091 ± 0.024	3.458 ± 0.539	3.627 ± 0.248	8.645 ± 0.937	10.307 ± 1.013	13.117 ± 1.046
16k		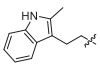	H	1.501 ± 0.176	16.159 ± 0.755	17.021 ± 1.112	>20	>20	>20
16l			H	0.084 ± 0.030	5.490 ± 0.740	4.085 ± 0.314	6.326 ± 0.801	6.282 ± 0.798	>20
16m	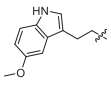		H	1.601 ± 0.742	16.563 ± 1.219	5.655 ± 0.257	>20	>20	3.220 ± 0.508
16n			H	0.322 ± 0.020	13.879 ± 1.142	1.902 ± 0.036	>20	>20	1.780 ± 0.250
16o	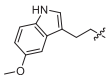		H	0.454 ± 0.051	14.339 ± 1.157	5.217 ± 0.054	11.101 ± 1.045	10.154 ± 1.007	1.780 ± 0.250
16p			$-CH_3$	0.707 ± 0.032	5.997 ± 0.778	4.018 ± 0.052	6.240 ± 0.795	6.416 ± 0.807	3.552 ± 0.551
16q	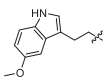	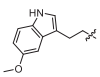	$-CH_3$	0.947 ± 0.086	6.480 ± 0.812	5.884 ± 0.413	4.016 ± 0.604	5.381 ± 0.371	4.510 ± 0.654

[a] Inhibitory activity was assayed by exposure various concentrations of the tested compounds for 72 h to substance and expressed as concentration required to inhibit tumor cell proliferation by 50% (IC_{50}). Data were presented as the means ± SDs. All experiments were carried out at least three independent times.

we tested the cell viability of PC3 cells treated with IC_{50} concentrations of represented compounds in the presence of Fe^{3+} by MTT assay. We can observe that the addition of Fe^{3+} resulted in more potent activity in comparison to compounds treatment alone, indicating that these compounds could be regarded as potential iron chelators (Fig. S1). To further evaluate the antiproliferative activity of compound **16f**, colony assay was performed. The results revealed that compound **16f** could obviously decrease colony formation both in PC3 and DU-145 cells, especially in the high dose groups, compared to the control groups (Fig. 3B and C).

2.2.3. *Effect of compound **16f** on cell cycle in PC3 and DU-145 cells*

Next, cell cycle assay was carried out to explore whether the antiproliferative activity of compound **16f** was related to cell cycle arrest in PC3 and DU-145 cells. PC3 and DU-145 cells treated with indicated concentrations of compound **16f** for 48 h were incubated

Table 3
The anticancer activity of synthetic derivatives against the tested cell lines.

Comp.	structure	IC_{50} (μM)[a]					
		PC3	EC109	DU-145	MGC803	MCF-7	WPMY-1
16f		0.054 ± 0.012	4.942 ± 0.694	1.439 ± 0.258	4.724 ± 0.674	5.334 ± 0.728	19.470 ± 1.242
16r	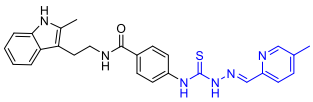	5.321 ± 0.263	9.499 ± 0.978	14.546 ± 0.064	>20	>20	2.870 ± 0.458
16s	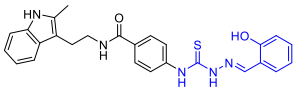	16.987 ± 0.178	>20	18.516 ± 0.125	>20	>20	>20
25	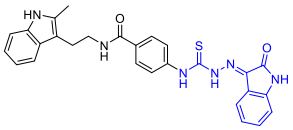	>20	>20	>20	>20	>20	>20
28	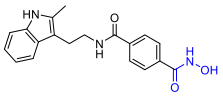	0.406 ± 0.091	0.664 ± 0.178	2.052 ± 0.145	4.219 ± 0.625	0.871 ± 0.062	0.450 ± 1.349
31	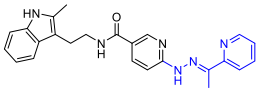	>20	>20	>20	>20	>20	>20
3-AP	–	0.560 ± 0.031	ND	ND	ND	ND	4.963 ± 0.020
DPC	–	0.122 ± 0.024	ND	ND	ND	ND	0.711 ± 0.152

[a] Inhibitory activity was assayed by exposure various concentrations of the tested compounds for 72 h to substance and expressed as concentration required to inhibit tumor cell proliferation by 50% (IC_{50}). Data were presented as the means ± SDs. All experiments were carried out at least three independent times.

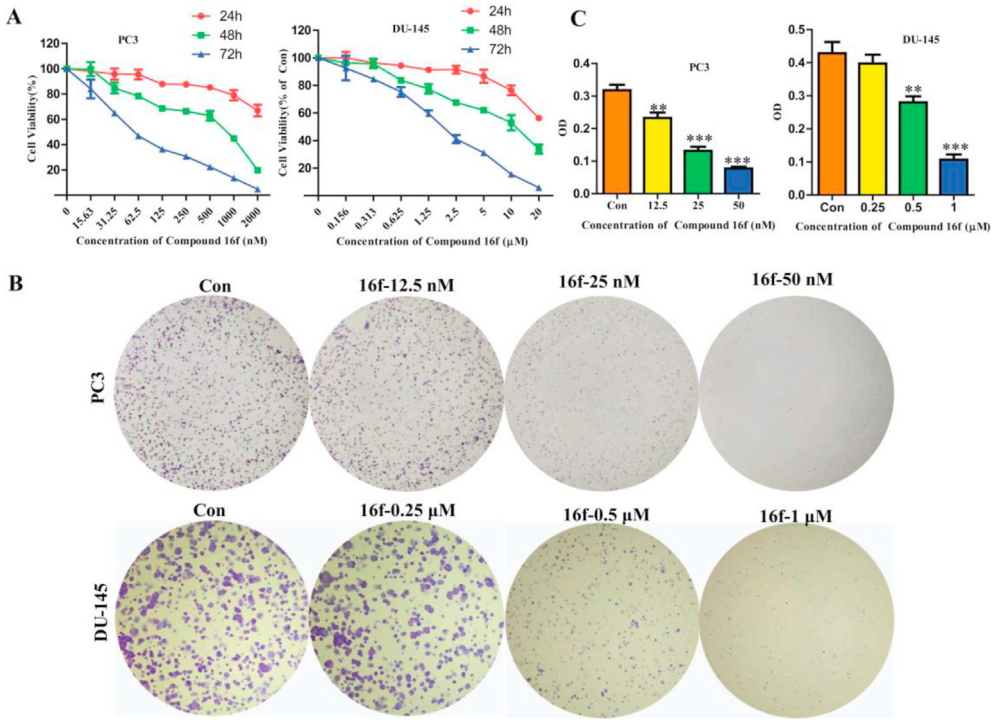

Fig. 3. A. Cell viability in PC3 and DU-145 cells treated with serial concentrations of compound **16f** for 24 h, 48 h and 72 h, respectively, by MTT assay. B. Representative pictures of colony formation stained by crystal violet in PC3 and DU-145 cells treated with indicated concentrations of compound **16f** for 6 days. C. The absorbance of crystal violet in PC3 and DU-145 cells measured at 570 nm. The data was presented as Mean ± SD. Three individual experiments were performed. *$p < 0.05$, **$p < 0.01$, ***$p < 0.001$ compared with the control (Con) group. (For interpretation of the references to color in this figure legend, the reader is referred to the Web version of this article.)

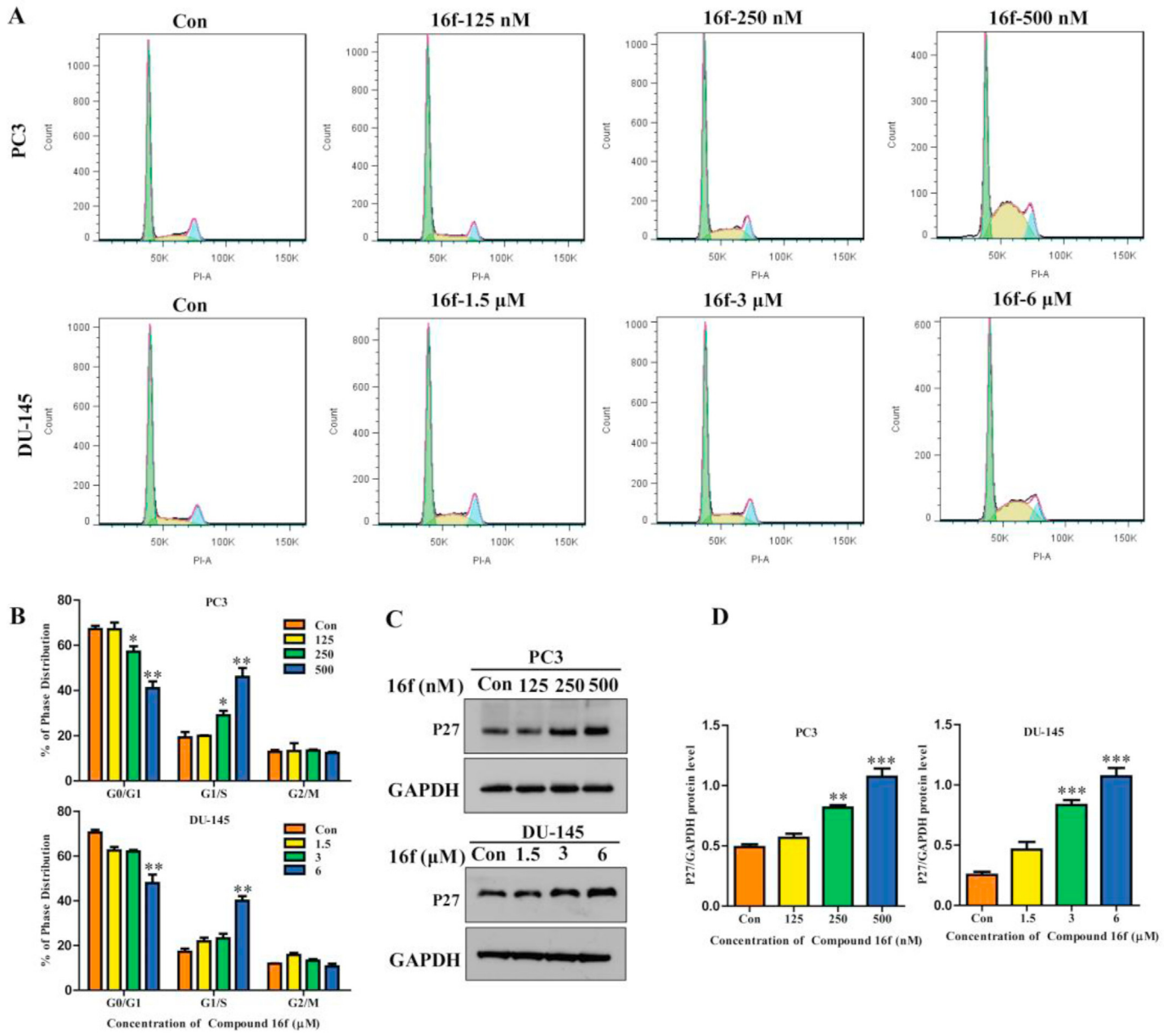

Fig. 4. A. Representative pictures of cell cycle in PC3 and DU-145 cells treated with compound **16f** at different concentrations for 48 h. B. Quantitative analysis of the percentages of cells cycle distribution in PC3 and DU-145 cells affected by compound **16f**. C-D. The Western blot analysis and quantitation of P27 protein in PC3 and DU-145 cells affected by indicated concentrations of compound **16f** for 48 h. The data was presented as Mean ± SD. Three individual experiments were performed. $*p < 0.05$, $**p < 0.01$, $***p < 0.001$ compared with the control (Con) group.

in PI staining buffer, and they were analyzed through flow cytometry. The results demonstrated that compound **16f** could induce G1/S cycle arrest as the concentrations of compound **16f** increased. The percentages of cells in the G1/S phase were increased from 19.23% to 19.98%, 29.04% and 49.02%, respectively in PC3 cells, compared to that in the control group. Similarly, compound **16f** also triggered G1/S cycle arrest in DU-145 cells dose-dependently (Fig. 4A, Fig. 4B). In addition, as an inhibitor of the cyclin-dependent kinase, P27 reflects the G1/S restriction [44]. Therefore, we further tested the protein levels of P27 in the PC3 and DU-145 cells treated with different concentrations of compound **16f** for 48 h by Western blot. As expected, the results displayed that P27 was significantly increased in PC3 and DU-145 cells affected by compound **16f** (Fig. 4C).

2.2.4. *Effect of compound **16f** on apoptosis in PC3 and DU-145 cells*

Moreover, Hoechst 33,342 staining was used to determine the pro-apoptotic ability of analogue **16f**. As shown in Fig. 5A, evident morphological changes, including cell rounding, formation of apoptotic bodies and nuclear fragmentation were presented and increased in the PC3 and DU-145 cells treated with compound **16f**. Next, we assessed cell apoptosis using Annexin V-FITC/PI double staining. Significant increase of positive cells was observed in PC3 and DU-145 cells, suggesting potential pro-apoptotic effects of compound **16f** (Fig. 5B and C). Death receptor signaling and mitochondrial control of apoptosis are the main pathways in the regulation of tumor apoptosis [45]. Thus, we investigated the expression of apoptosis-related proteins in PC3 and DU-145 cells treated with different concentrations of compound **16f** by Western blot (Fig. 5D and E). The results exhibited that the expression of anti-apoptotic

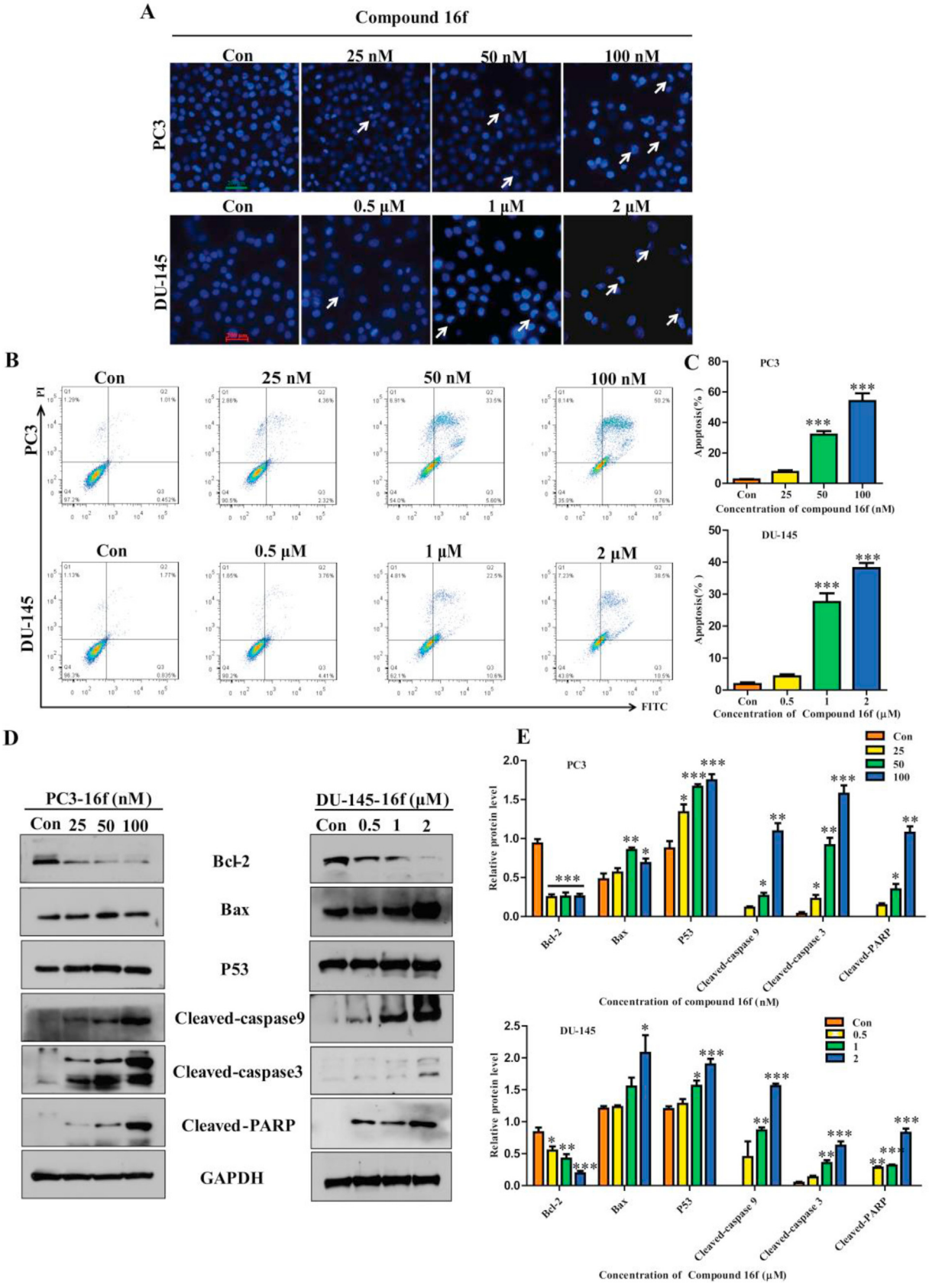

Fig. 5. A. Hoechst 33,342 staining in PC3 and DU-145 cells treated with different concentrations of compound **16f** for 72 h (changes in cell morphology marked with red arrows). B. Representative pictures of apoptotic distributions in PC3 and DU-145 cells affected by compound **16f** at indicated concentrations for 72 h by Annexin V-FITC/PI double staining. C. The quantitative analysis of apoptotic rates at both early and advanced stages of PC3 and DU-145 cells by flow cytometry. D. The Western blot analysis of the apoptosis-related proteins. F. The quantitative analysis of the protein levels. The data was presented as Mean ± SD. Three individual experiments were performed. $*p < 0.05$, $**p < 0.01$, $***p < 0.001$ compared with the control (Con) group. (For interpretation of the references to color in this figure legend, the reader is referred to the Web version of this article.)

protein Bcl-2 was markedly reduced, while pro-apoptotic protein Bax was increased. Simultaneously, the expression of cleaved caspase 9/3 and PARP exhibited a significant elevation in a concentration-dependent manner. Additionally, compound **16f** promoted the expression of P53 in PC3 and DU-145 cells. Taken together, these finding suggested that compound **16f** could induce human prostatic cancer PC3 and DU-145 cell apoptosis potentially *via* both the death receptor and mitochondria-mediated pathways.

2.2.5. Effect of compound 16f on reactive oxygen species (ROS) in PC3 and DU-145 cells

Excess accumulation of ROS in cells can lead to oxidative stress damage and tumor cell death, and contribute to enhancing cell cycle arrest and apoptosis [46,47]. In addition, the anticancer activity of TSCs was associated with their ability to generate ROS in a Fenton and Haber-Weiss reaction [23,30,34]. In order to explore the potential mechanism of compound **16f** induced cell cycle arrest and apoptosis, we detected the intracellular ROS level in PC3 and DU-145 cells treated with compound **16f** by flow cytometry (Fig. 6A). The results suggested that compound **16f** could dose-dependently increase ROS production both in PC3 and DU-145 cells (Fig. 6B). Importantly, pretreatment with 5 mM of NAC, a strong antioxygen, obviously alleviated the intracellular level of ROS induced by compound **16f** stimulation (Fig. 6C and D). To further understand the potential mechanism underlying the accumulation of intracellular ROS induced by compound **16f** in PC3 and DU-145 cells, MAPK signaling pathway was analyzed. As shown in Fig. 6E, the MAPK signaling pathway was activated by compound **16f**. The phosphorylation levels of ERK1/2 (Thr202/Tyr204), JNK (Thr183/Tyr185) and P38 (Thr180/Tyr182) were significantly increased in response to compound **16f** treatment. In addition, the statistical analysis of the Western blot revealed an obvious elevation in the p-JNK/JNK, p-P38/P38 and p-ERK/ERK ratios in compound **16f** treatment groups, compared to those in the control (Con) groups (Fig. 6F). Of note, p-JNK and p-ERK are known mediators of cell proliferation and inhibition of apoptosis [48]. Moreover, nuclear P27, increased by compound **16f** in PC3 and DU-145 cells (Fig. 4C), can effectively regulate MAPK pathway [49]. In order to further verify whether P38 MAPK pathway participated in the compound **16f**-induced apoptosis, PC3 and DU-145 cells were pretreated with 4 mM P38 inhibitor SB203580 for 4 h, followed by treatment with the IC_{50} concentration of compound **16f** for 72 h, respectively, by MTT assay. Expectedly, the results displayed that the P38 inhibitor (SB203580) effectively improved the cell viability in PC3 and DU-145 cells treated with compound **16f**, respectively, suggesting that P38 MAPK pathway indeed played an important role in the compound **16f**-induced apoptosis (Fig. 6G). In general, the above results suggested that compound **16f** resulted in high levels of ROS by activating the MAPK signaling pathway in PC3 and DU-145 cells, which may be related to cell cycle arrest and apoptosis.

*2.2.6. Safety evaluation of compound **16f** in vivo*

The potential side effects have limited clinical utility of thiosemicarbazone derivatives to some extent [8]. Given highly antiproliferative activity and selectivity toward PC3 cells, acute toxicity test was performed to evaluate the safety of compound **16f** *in vivo*. Mice were administrated intragastrically at a dosage of 2 g/kg at a time, and then they were fed normally and observed for two weeks. During this time, not only the mice in the **16f** treated group survived, but they maintained their weight without any noticeable behavioral abnormalities (Fig. 7A). In addition, H&E staining demonstrated that compound **16f** showed no signs of toxicity in the heart, liver, spleen, lung and kidney, compared to the control group (Fig. 7B). These data revealed that compound **16f** had no obvious toxicity and side effect *in vivo*.

*2.2.7. Antitumor studies of compound **16f** on xenograft model bearing PC3 cells*

Given the potent antiproliferative and pro-apoptotic activity of compound **16f** toward prostate cancer cells *in vitro*, we then further investigated the antitumor effect of **16f** *in vivo* through a xenograft model bearing PC3 cells. The corresponding solvent and 3-AP were used as negative and positive controls, respectively. The mouse body weight and tumor volume were measured every 2 days. The results demonstrated that compound **16f** treatment at 12.5 mg/kg and 25 mg/kg significantly alleviated the tumor volume, compared to that in the negative control group (Fig. 8A, Fig. 8B). The average tumor weight in compound **16f** treatment group mice was decreased to 53.6% and 43.4%, respectively (Fig. 8C). In addition, in comparison to 3-AP, compound **16f** displayed similar inhibitory effect in the same concentration. Besides, compound **16f** did not result in obvious side effects in the body weight and general health, compared to the negative control mice (Fig. 8D). These data indicated that compound **16f** could effectively inhibit tumor growth through a xenograft model bearing PC3 cells.

3. Conclusions

In summary, we have designed and synthesized a variety of new thiosemicarbazone derivatives and carried out systematic SAR research. Particularly, we found that introduction of benzamide group into the linker was beneficial to anticancer activity and selectivity. Additionally, replacement NNS donor with other donor chelators resulted in significantly decreased potency, suggesting that NNS donor was responsible for antiproliferative activity. Besides, most described compounds displayed strong biological activity against prostate cancer PC3 cells. The most promising molecule **16f** was confirmed potent activity and high selectivity toward PC3 cells, as well as no obvious toxicity *in vivo* and *in vitro*. Preliminary mechanism studies revealed that compound **16f** effectively inhibited colony formation in PC3 and DU-145 cells. Also, G1/S cycle arrest and apoptosis were induced by derivative **16f**, which may be linked to ROS-mediated MAPK pathways. More importantly, analogue **16f** could significantly suppress tumor growth in the xenograft model bearing PC3 cells. Our findings highlight thiosemicarbazone derivative **16f** as a promising compound for further study regarding novel anti-prostate cancer therapies.

4. Experimental section

4.1. General

We determined melting points of all analogues using the WRS-1A digital melting point apparatus. Thin-layer chromatography (TLC) was performed on the glass pane that painted with silica gel, visualized by 254 nm ultraviolet lamp. All chemicals and solvents were obtained from commercial sources and used without further purification. High resolution mass spectra (HRMS) were recorded on a Waters Micromass Q-T of Micromass spectrometer by electrospray ionizaton (ESI). NMR spectra were recorded on a Bruker 400 MHz spectrometer (400 and 100 MHz for the ^{1}H and ^{13}C nuclei, respectively) using DMSO as solvent from commercial sources. The purity of all compounds was examined by reverse-phase high-performance liquid chromatography (HPLC) analysis. The signal was monitored at 287 nm with a UV detector. A flow rate of 1.0 mL/min was used with a mobile phase of MeOH in H_2O (90:10, v/v). The data in this study was analyzed by one-way analysis of variance, and the results were expressed as mean ± standard deviation (SD). $P < 0.05$ was considered statistically significant.

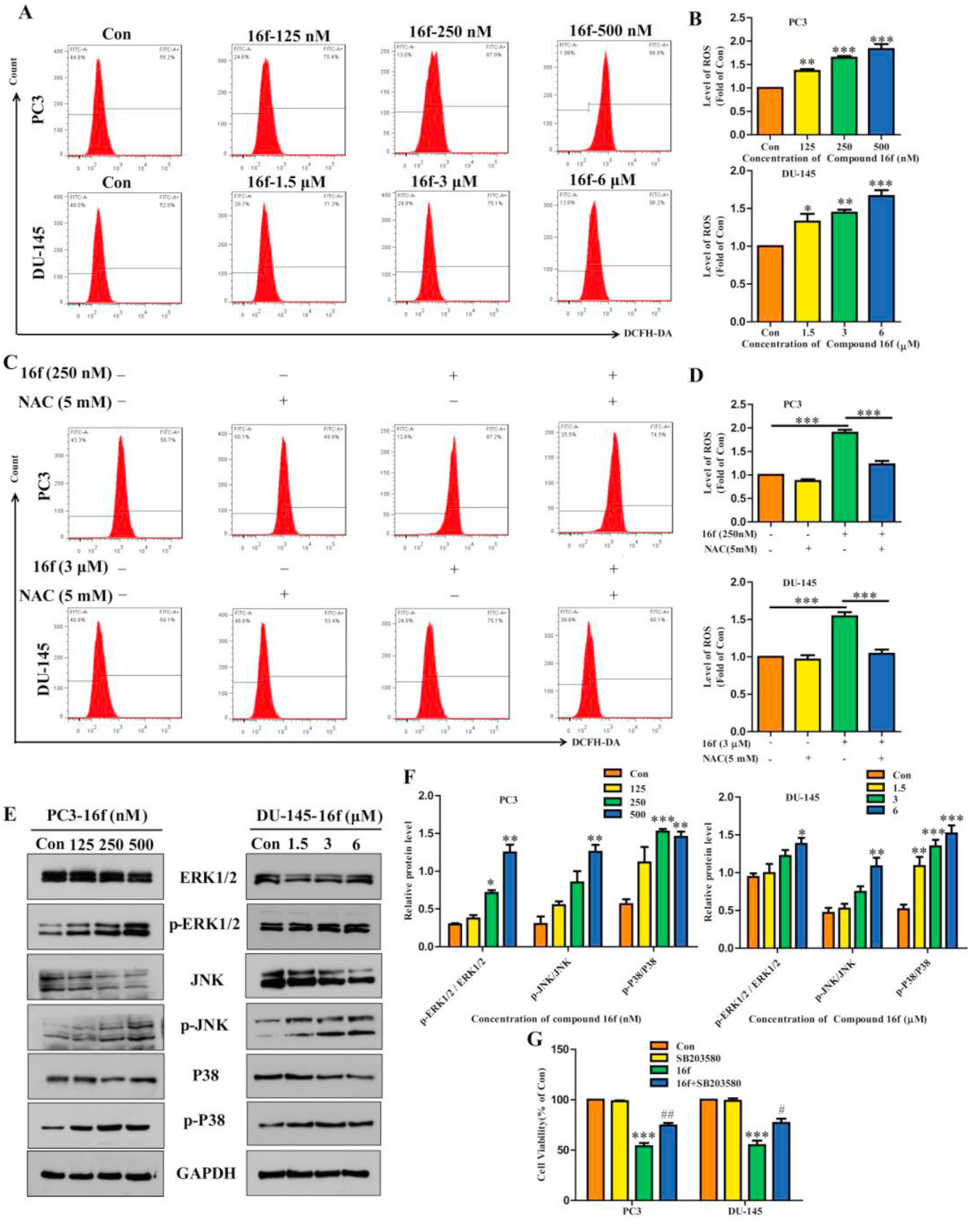

Fig. 6. A. Representative images of ROS production in PC3 and DU-145 cells treated with analogue **16f** at different concentrations for 48 h by DCFH-DA staining. B. The quantitative analysis of ROS levels in PC3 and DU-145 cells affected by compound **16f** through flow cytometry. C. Representative images of ROS production in PC3 and DU-145 cells treated with

4.2. General procedure for the synthesis of compound(4)

To a solution of commercially available **1** (3.125 mmol) in anhydrous ethanol (18 mL) was added triethylamine (6.25 mmol) and CS_2 (6.25 mmol). The mixture was stirred at room temperature for 3 h. Upon completion, then DMAP (0.425 mmol) and Boc_2O (8.5 mmol) were added, and the reaction mixture was stirred at room temperature for another 0.5 h. The solvent was distilled off and extracted with ethyl acetate. The combined organics were dried and evaporated to dryness. Purification by silica chromatography afforded intermediate **2** as a colorless liquid. A mixture of **2** (2.5 mmol) and hydrazine hydrate (7.5 mmol) in dichloromethane (15 mL) was stirred under at room temperature for 2 h. The precipitated solid was filtered off and washed with dichloromethane to give the title compound **3** as white solid. To the solution of **3** (0.64 mmol) in ethanol containing 5-methylpicolinaldehyde (0.77 mmol), catalytic amount acetic acid (0.064 mmol) was added. The reaction mixture was stirred at room temperature for 2 h. Upon completion, formed precipitation was filtered washed with ethanol to provide derivative **4** as yellow solid in 69% yield.

4.2.1. (E)-N-(2-(1H-indol-3-yl)ethyl)-2-((5-methylpyridin-2-yl) methylene)hydrazine-1-carbothioamide (**4**)

Yellow solid, m. p. 178.7–180.4 °C, yield 69%, purity 98.63%. ^{1}H NMR (400 MHz, DMSO-d_6, ppm) δ 11.68 (s, 1H), 10.86 (s, 1H), 8.69 (dd, J = 20.2, 14.7 Hz, 1H), 8.41 (s, 1H), 8.08 (s, 1H), 8.05 (d, J = 8.1 Hz, 1H), 7.73 (d, J = 7.8 Hz, 1H), 7.68 (d, J = 7.9 Hz, 1H), 7.36 (d, J = 8.0 Hz, 1H), 7.22 (s, 1H), 7.08 (t, J = 7.4 Hz, 1H), 6.99 (t, J = 7.4 Hz, 1H), 3.85 (dd, J = 14.1, 6.5 Hz, 2H), 3.10–2.94 (m, 2H), 2.33 (s, 3H). ^{13}C NMR (100 MHz, DMSO-d_6, δ, ppm) δ 177.00, 150.64, 149.53, 142.21, 136.95, 136.26, 133.74, 127.24, 122.65, 121.00, 119.59, 118.53, 118.26, 111.53, 111.36, 44.36, 24.79, 17.89. HR-MS (ESI), calcd. $C_{18}H_{19}N_5S$, $[M+H]^+m/z$: 338.1439. Found: 338.1435.

4.3. General procedure for the synthesis of compound(9)

A mixture of raw materials **1** (20 mmol), 4-aminocyclohexane-1-carboxylic acid (20 mmol), EDCI (20 mmol) and HOBT (20 mmol) in dichloromethane (100 mL) were stirred at room temperature for 6 h. Upon completion of the reaction indicated by TLC, the mixture was extracted with DCM for two times. The combined organic layers were evacuated to afford the residue, which was then purified by chromatography (silica gel, 5% methanol/dichloromethane) to obtain intermediate **6** as a white solid. Compound **9** was synthesized from intermediate **6**, according to our previously reported methods in 32% yields [39].

4.3.1. N-(2-(1H-indol-3-yl)ethyl)-4-(hydrazinecarbothioamido) cyclohexane-1-carboxamide (**8**)

Yellow solid, m. p. 160.4–161.2 °C, yield 38%. ^{1}H NMR (400 MHz, DMSO-d_6, ppm) δ 10.78 (s, 1H), 8.66 (s, 1H), 7.85 (s, 1H), 7.68 (s, 1H), 7.54 (d, J = 7.8 Hz, 1H), 7.33 (d, J = 8.1 Hz, 1H), 7.19–6.90 (m, 3H), 4.54 (s, 2H), 4.29 (s, 1H), 3.31 (s, 2H), 2.81 (t, J = 7.1 Hz, 2H), 2.20 (s, 1H), 1.79–1.46 (m, 8H). ^{13}C NMR (100 MHz, DMSO-d_6, δ, ppm) δ 174.35, 136.19, 127.22, 122.57, 120.85, 118.25, 118.14, 111.86, 111.31, 47.79, 41.50, 29.01, 25.21, 24.78. HR-MS (ESI), calcd. $C_{18}H_{25}N_5OS$, $[M+H]^+m/z$: 360.1858. Found: 360.1850.

4.3.2. (E)-N-(2-(1H-indol-3-yl)ethyl)-4-(2-((5-methylpyridin-2-yl) methylene)hydrazine-1-carbothioamido)cyclohexane-1-carboxamide (**9**)

Yellow solid, m. p. 210.1–213.4 °C, yield 32%, purity 95.05%. ^{1}H NMR (400 MHz, DMSO-d_6, ppm) δ 11.66 (s, 1H), 10.80 (s, 1H), 8.41 (s, 1H), 8.15–7.99 (m, 3H), 7.86 (s, 1H), 7.66 (d, J = 7.5 Hz, 1H), 7.56 (d, J = 7.6 Hz, 1H), 7.33 (d, J = 8.0 Hz, 1H), 7.14 (s, 1H), 7.06 (t, J = 7.3 Hz, 1H), 6.98 (t, J = 7.3 Hz, 1H), 4.30 (s, 1H), 3.34 (s, 4H), 2.84 (t, J = 7.1 Hz, 2H), 2.31 (s, 4H), 1.83 (d, J = 7.2 Hz, 4H), 1.61 (d, J = 39.7 Hz, 4H). ^{13}C NMR (100 MHz, DMSO-d_6, δ, ppm) δ 175.35, 174.12, 150.47, 149.60, 142.64, 137.01, 136.21, 133.81, 127.46, 127.23, 122.56, 120.85, 119.67, 118.25, 118.13, 111.90, 111.32, 50.81, 28.35, 25.67, 25.31, 17.89. HR-MS (ESI), calcd. $C_{25}H_{30}N_6OS$, $[M+H]^+m/z$: 463.2280. Found: 463.2272.

4.4. General procedure for the synthesis of compound(16a-s)

To a solution of **10a-e** (15 mmol) and **11a**-**b** (15 mmol) in dry dichloromethane (100 mL) were added EDCI (15 mmol) and HOBT (15 mmol) at room temperature. The reaction was monitored by TLC. After 6 h stirring at room temperature, H_2O was added. The aqueous layer was extracted twice with dichloromethane. The combined organic layers were concentrated and purified by flash chromatography on silica gel (5% methanol/dichloromethane) to give the intermediates **12a-f** as solid. A mixture of **12a-f** (10 mmol) and 10% Pd/C (2.2 mmol) in methanol (70 mL) was stirred under an atmosphere of H_2 at room temperature for 6 h. Upon completion, the reaction mixture was filtered, and the filtrate was evaporated to dryness. Then, the residue was purified by chromatography on silica gel (10% methanol/dichloromethane) to obtain **13a-f** as solid. Derivatives **16a-s** were synthesized from intermediates **13a-f** according to our previously reported methods in 35–65% yields [39].

4.4.1. N-(2-(1H-indol-3-yl)ethyl)-4-(hydrazinecarbothioamido) benzamide (**15a**)

Yellow solid, m. p. 150.6–152.5 °C, yield 54%. ^{1}H NMR (400 MHz, DMSO-d_6, ppm) δ 10.80 (s, 1H), 9.29 (s, 1H), 8.50 (s, 1H), 7.80 (dd, J = 15.0, 8.4 Hz, 4H), 7.59 (d, J = 7.8 Hz, 1H), 7.34 (d, J = 8.0 Hz, 1H), 7.18 (d, J = 1.9 Hz, 1H), 7.07 (t, J = 7.5 Hz, 1H), 6.98 (t, J = 7.4 Hz, 1H), 4.89 (s, 2H), 3.54 (dd, J = 13.6, 6.9 Hz, 2H), 2.95 (t, J = 7.5 Hz, 2H). ^{13}C NMR (100 MHz, DMSO-d_6, δ, ppm) δ 165.72, 136.20, 127.25, 127.13, 122.57, 122.15, 120.90, 118.28, 118.21, 111.91, 111.34, 40.15, 25.19. HR-MS (ESI), calcd. $C_{18}H_{19}N_5OS$, $[M+H]^+m/z$: 354.1388. Found: 354.1381.

4.4.2. N-(2-(1H-indol-3-yl)ethyl)-6-(hydrazinecarbothioamido) nicotinamide (**15b**)

Yellow solid, m. p. 168.1–169.4 °C, yield 43%. ^{1}H NMR (400 MHz, DMSO-d_6, ppm) δ 10.81 (s, 1H), 9.51 (s, 1H), 8.83 (d, J = 30.4 Hz, 2H), 8.37 (s, 1H), 7.97 (d, J = 8.3 Hz, 1H), 7.62 (d, J = 7.7 Hz, 1H), 7.34 (d, J = 8.0 Hz, 1H), 7.19 (s, 1H), 7.07 (t, J = 7.3 Hz, 1H), 6.98 (t, J = 7.4 Hz, 1H), 3.59 (d, J = 6.6 Hz, 2H), 2.96 (t, J = 7.2 Hz, 2H). ^{13}C NMR (100 MHz, DMSO-d_6, δ, ppm) δ 179.49, 163.49, 143.45, 136.25, 131.08, 127.22, 124.50, 122.54, 121.10, 120.92, 118.38, 118.19, 111.76, 111.32, 25.29. HR-MS (ESI), calcd. $C_{17}H_{18}N_6OS$, $[M+H]^+m/z$: 355.1341. Found: 355.1333.

compound **16f** for 48 h in the presence or absence of NAC (5 mM). D. The quantitative analysis of ROS levels in PC3 and DU-145 cells affected by compound **16f** for 48 h in the presence or absence of NAC (5 mM) through flow cytometry. E. The Western blot analysis of ERK1/2, p-ERK1/2, JNK, p-JNK, P38 and p-P38 in PC3 and DU-145 cells treated with indicated concentrations of compound **16f**. F. The quantitative analysis of these protein levels in PC3 and DU-145 cells affected by compound **16f**. G. Cell viability in PC3 and DU-145 cells pretreated with 4 mM p38 inhibitor SB203580 for 4 h, respectively, followed by treatment with the IC_{50} concentrations of compound **16f** for 72 h, respectively, by MTT assay. The data was presented as Mean ± SD. Three individual experiments were performed. *p < 0.05, **p < 0.01, ***p < 0.001 compared with the control (Con) group, #p < 0.05, ##p < 0.01 compared with the compound **16f** group.

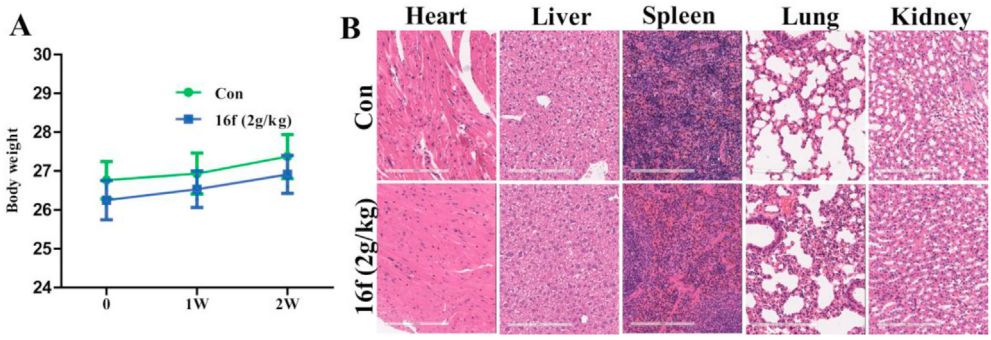

Fig. 7. A. The weight gain of the mice intragastrically administrated with compound **16f** or control oil. B. The representative H&E staining of the major tissue sections from compound **16f** treated and control mice. n = 10 per group.

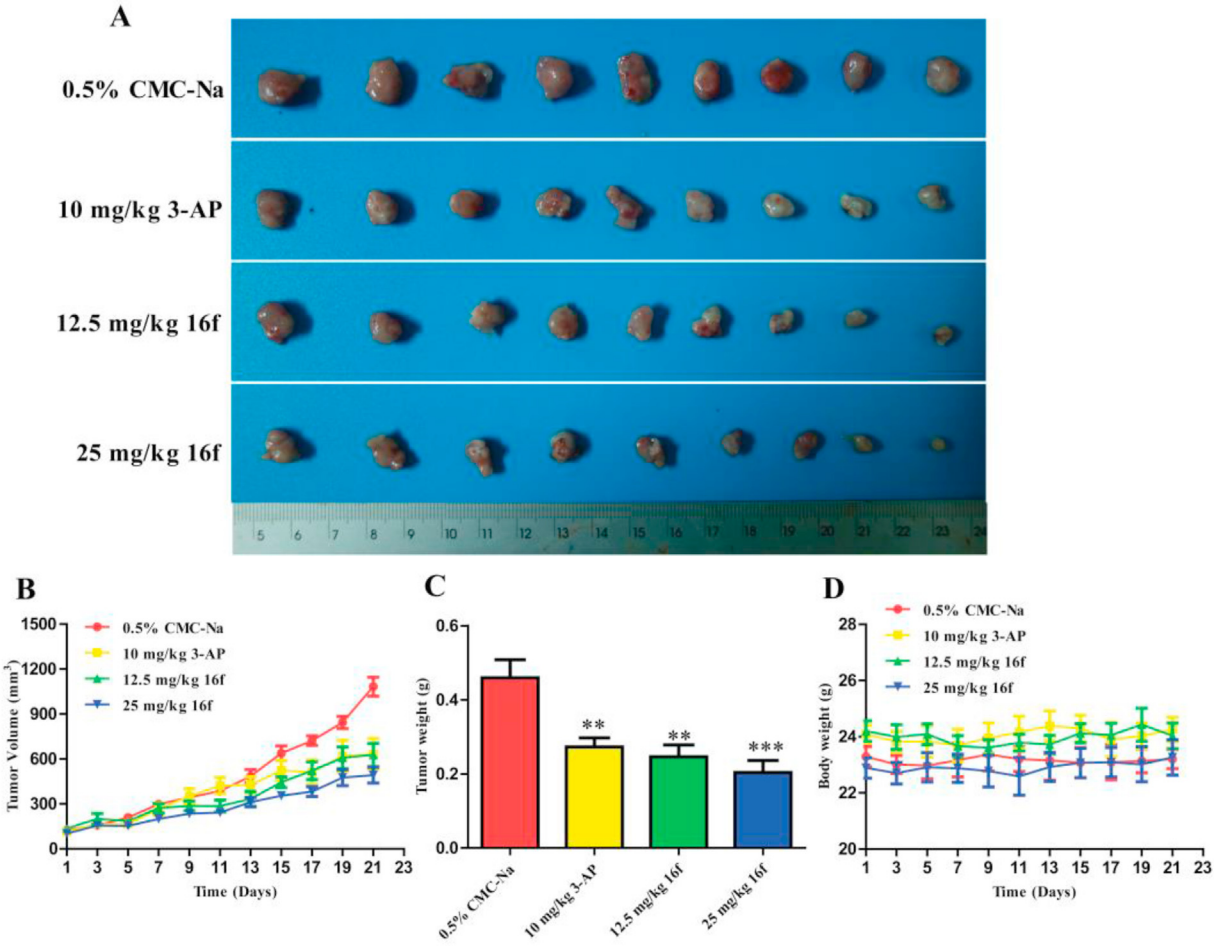

Fig. 8. PC3 cells were transplanted subcutaneously to the right sides of BALB/C-NU mice and subjected to 0.5% CMC-Na, 3-AP (10 mg/kg) and **16f** (12.5 and 25 mg/kg), respectively, for 21 days. A. Images of tumors. B. Tumor volume. C. Final tumor weight. D. Body weight in each group. The data was presented as Mean ± SD. n = 9 per group. $^{**}p < 0.01$, $^{***}p < 0.001$ compared with the 0.5% CMC-Na group.

*4.4.3. N-(2-(5-chloro-1H-indol-3-yl)ethyl)-4-(hydrazinecarbothioamido)benzamide (**15c**)*

White solid, m. p. 148.7–149.1 °C, yield 45%. ^{1}H NMR (400 MHz, DMSO-d_6, ppm) δ 11.02 (s, 1H), 9.29 (s, 1H), 8.50 (s, 1H), 7.79 (t, J = 13.6 Hz, 4H), 7.63 (s, 1H), 7.35 (d, J = 8.5 Hz, 1H), 7.27 (s, 1H), 7.06 (d, J = 7.4 Hz, 1H), 4.87 (s, 2H), 3.51 (d, J = 6.1 Hz, 2H), 2.93 (t, J = 7.2 Hz, 2H). ^{13}C NMR (100 MHz, DMSO-d_6, δ, ppm) δ 165.70, 134.66, 128.47, 127.12, 124.59, 122.97, 120.79, 117.61, 112.87, 111.96, 40.13, 24.98. HR-MS (ESI), calcd. $C_{18}H_{18}ClN_5OS$, $[M+H]^+ m/z$: 388.0999. Found: 388.0999.

*4.4.4. 4-(hydrazinecarbothioamido)-N-(2-(5-methyl-1H-indol-3-yl)ethyl)benzamide (**15d**)*

White solid, m. p. 166.2–167.5 °C, yield 42%. ^{1}H NMR (400 MHz, DMSO-d_6, ppm) δ 10.65 (s, 1H), 9.29 (s, 1H), 8.48 (s, 1H), 7.80 (dd, J = 14.8, 8.5 Hz, 4H), 7.35 (s, 1H), 7.22 (d, J = 8.2 Hz, 1H), 7.09 (d,

J = 20.2 Hz, 1H), 6.89 (d, *J* = 8.2 Hz, 1H), 4.86 (s, 2H), 3.52 (dd, *J* = 13.6, 6.6 Hz, 2H), 2.92 (t, *J* = 7.4 Hz, 2H), 2.36 (s, 3H). ^{13}C NMR (100 MHz, DMSO-d_6, δ, ppm) δ 165.63, 134.61, 127.52, 127.14, 126.53, 122.68, 122.46, 122.14, 117.94, 111.43, 111.04, 40.28, 25.23, 21.25. HR-MS (ESI), calcd. $C_{19}H_{21}N_5OS$, $[M+H]^+m/z$: 368.1545. Found: 368.1538.

*4.4.5. 4-(hydrazinecarbothioamido)-N-(2-(5-methoxy-1H-indol-3-yl)ethyl)benzamide (**15e**)*

Yellow solid, m. p. 166.2–167.4 °C, yield 48%. ^{1}H NMR (400 MHz, DMSO-d_6, ppm) δ 10.62 (s, 1H), 9.27 (s, 1H), 8.48 (s, 1H), 7.80 (d, *J* = 10.8 Hz, 4H), 7.22 (d, *J* = 8.7 Hz, 1H), 7.10 (d, *J* = 30.0 Hz, 2H), 6.71 (d, *J* = 8.3 Hz, 1H), 4.89 (s, 2H), 3.73 (s, 3H), 3.53 (d, *J* = 5.7 Hz, 2H), 2.92 (t, *J* = 6.9 Hz, 2H). ^{13}C NMR (100 MHz, DMSO-d_6, δ, ppm) δ 165.64, 152.95, 131.35, 127.61, 127.12, 124.50, 123.25, 122.10, 111.96, 111.77, 111.04, 100.16, 55.28, 40.13, 25.21. HR-MS (ESI), calcd. $C_{19}H_{21}N_5O_2S$, $[M+H]^+m/z$: 384.1494. Found: 384.1487.

*4.4.6. 4-(hydrazinecarbothioamido)-N-(2-(2-methyl-1H-indol-3-yl)ethyl)benzamide (**15f**)*

Yellow solid, m. p. 164.9–165.7 °C, yield 50%. ^{1}H NMR (400 MHz, DMSO-d_6, ppm) δ 10.71 (s, 1H), 9.30 (s, 1H), 8.51 (s, 1H), 7.79 (t, *J* = 12.9 Hz, 4H), 7.48 (d, *J* = 7.5 Hz, 1H), 7.23 (d, *J* = 7.6 Hz, 1H), 6.95 (dt, *J* = 14.8, 6.7 Hz, 2H), 4.88 (s, 2H), 3.40 (d, *J* = 6.6 Hz, 2H), 2.88 (t, *J* = 7.2 Hz, 2H), 2.31 (s, 3H). ^{13}C NMR (100 MHz, DMSO-d_6, δ, ppm) δ 165.64, 135.20, 132.05, 128.36, 127.11, 122.06, 119.88, 118.06, 117.31, 110.34, 107.70, 40.31, 24.15, 11.19. HR-MS (ESI), calcd. $C_{19}H_{21}N_5OS$, $[M+H]^+m/z$: 368.1545. Found: 368.1538.

*4.4.7. (E)-N-(2-(1H-indol-3-yl)ethyl)-4-(2-((5-methylpyridin-2-yl)methylene)hydrazine-1-carbothioamido)benzamide (**16a**)*

White solid, m. p. 204.1–205.4 °C, yield 65%, purity 98.45%. ^{1}H NMR (400 MHz, DMSO-d_6, ppm) δ 12.09 (s, 1H), 10.81 (s, 1H), 10.31 (s, 1H), 8.67–8.50 (m, 1H), 8.44 (s, 1H), 8.35 (d, *J* = 8.1 Hz, 1H), 8.20 (s, 1H), 7.85 (dd, *J* = 17.8, 7.3 Hz, 2H), 7.71 (dd, *J* = 14.6, 8.4 Hz, 3H), 7.60 (d, *J* = 7.8 Hz, 1H), 7.35 (d, *J* = 8.1 Hz, 1H), 7.20 (s, 1H), 7.08 (t, *J* = 7.4 Hz, 1H), 6.99 (t, *J* = 7.4 Hz, 1H), 3.56 (dd, *J* = 13.4, 6.9 Hz, 2H), 2.97 (t, *J* = 7.4 Hz, 2H), 2.34 (s, 3H). ^{13}C NMR (100 MHz, DMSO-d_6, δ, ppm) δ 175.97, 165.64, 150.46, 149.59, 143.63, 141.40, 136.91, 136.23, 134.06, 131.31, 127.28, 127.07, 124.88, 122.59, 120.89, 120.21, 118.28, 118.20, 111.92, 111.35, 25.20, 17.93. HR-MS (ESI), calcd. $C_{25}H_{24}N_6OS$, $[M+Na]^+m/z$: 479.1630. Found: 479.1627.

*4.4.8. (E)-N-(2-(1H-indol-3-yl)ethyl)-6-(2-((5-methylpyridin-2-yl)methylene)hydrazine-1-carbothioamido)nicotinamide (**16b**)*

White solid, m. p. 187.2–188.4 °C, yield 43%, purity 97.19%. ^{1}H NMR (400 MHz, DMSO-d_6, ppm) δ 12.29 (s, 1H), 10.82 (s, 1H), 10.47 (s, 1H), 8.94–8.69 (m, 2H), 8.45 (s, 1H), 8.35 (d, *J* = 8.1 Hz, 1H), 8.22 (d, *J* = 8.7 Hz, 2H), 8.12–7.98 (m, 1H), 7.72 (d, *J* = 8.0 Hz, 1H), 7.63 (d, *J* = 7.8 Hz, 1H), 7.35 (d, *J* = 8.1 Hz, 1H), 7.21 (s, 1H), 7.08 (t, *J* = 7.3 Hz, 1H), 6.99 (t, *J* = 7.3 Hz, 1H), 3.62 (d, *J* = 6.5 Hz, 2H), 2.99 (t, *J* = 7.2 Hz, 2H), 2.34 (s, 3H). ^{13}C NMR (100 MHz, DMSO-d_6, δ, ppm) δ 176.53, 163.37, 150.33, 149.66, 146.41, 145.50, 144.22, 138.04, 136.93, 136.25, 134.22, 133.86, 127.23, 122.57, 121.31, 120.93, 120.21, 118.39, 118.20, 111.75, 111.62, 25.27, 17.94. HR-MS (ESI), calcd. $C_{24}H_{23}N_7OS$, $[M+H]^+m/z$: 458.1763. Found: 458.1755.

*4.4.9. (E)-N-(2-(5-chloro-1H-indol-3-yl)ethyl)-4-(2-((5-methylpyridin-2-yl)methylene)hydrazine-1-carbothioamido)benzamide (**16c**)*

Yellow solid, m. p. 203.4–204.5 °C, yield 61%, purity 96.48%. ^{1}H NMR (400 MHz, DMSO-d_6, δ, ppm) δ 12.09 (s, 1H), 11.03 (s, 1H), 10.31 (s, 1H), 8.60 (s, 1H), 8.44 (s, 1H), 8.35 (d, *J* = 8.1 Hz, 1H), 8.21 (s, 1H), 7.86 (dd, *J* = 8.4, 4.8 Hz, 2H), 7.72 (dd, *J* = 15.8, 8.5 Hz, 3H), 7.67–7.58 (m, 1H), 7.36 (t, *J* = 6.6 Hz, 1H), 7.28 (s, 1H), 7.07 (d, *J* = 8.3 Hz, 1H), 3.55 (dd, *J* = 12.7, 5.8 Hz, 2H), 3.03–2.89 (m, 2H), 2.34 (s, 3H). ^{13}C NMR (100 MHz, DMSO-d_6, δ, ppm) δ 175.97, 165.69, 150.46, 149.58, 143.63, 141.41, 136.91, 136.24, 134.68, 134.05, 131.28, 128.49, 127.06, 124.86, 124.60, 123.00, 122.58, 120.89, 120.80, 120.20, 118.28, 118.20, 117.61, 112.88, 111.97, 111.92, 111.35, 25.21, 24.96, 17.93. HR-MS (ESI), calcd. $C_{25}H_{23}ClN_6OS$, $[M+H]^+m/z$: 491.1421. Found: 491.1413.

*4.4.10. (E)-N-(2-(5-methyl-1H-indol-3-yl)ethyl)-4-(2-((5-methylpyridin-2-yl)methylene)hydrazine-1-carbothioamido)benzamide (**16d**)*

Yellow solid, m. p. 197.1–198.5 °C, yield 54%, purity 98.24%. ^{1}H NMR (400 MHz, DMSO-d_6, ppm) δ 12.09 (s, 1H), 10.65 (d, *J* = 12.4 Hz, 1H), 10.31 (s, 1H), 8.58 (t, *J* = 5.5 Hz, 1H), 8.44 (s, 1H), 8.35 (d, *J* = 8.1 Hz, 1H), 8.21 (s, 1H), 7.87 (d, *J* = 8.5 Hz, 2H), 7.72 (dd, *J* = 14.6, 8.4 Hz, 2H), 7.37 (s, 1H), 7.23 (d, *J* = 8.2 Hz, 1H), 7.14 (d, *J* = 1.7 Hz, 1H), 6.90 (d, *J* = 8.2 Hz, 1H), 3.54 (dd, *J* = 13.4, 7.0 Hz, 2H), 2.94 (t, *J* = 7.4 Hz, 2H), 2.37 (t, *J* = 13.7 Hz, 6H). ^{13}C NMR (100 MHz, DMSO-d_6, δ, ppm) δ 175.97, 165.63, 150.46, 149.59, 143.63, 141.39, 136.91, 134.62, 134.05, 131.34, 127.54, 127.07, 126.56, 124.86, 122.69, 122.48, 120.20, 117.94, 111.43, 111.05, 40.36, 25.21, 21.27, 17.93. HR-MS (ESI), calcd. $C_{26}H_{26}N_6OS$, $[M+H]^+m/z$: 471.1967. Found: 471.1959.

*4.4.11. (E)-N-(2-(5-methoxy-1H-indol-3-yl)ethyl)-4-(2-((5-methylpyridin-2-yl)methylene)hydrazine-1-carbothioamido)benzamide (**16e**)*

White solid, m. p. 200.4–203.1 °C, yield 58%, purity 96.93%. ^{1}H NMR (400 MHz, DMSO-d_6, ppm) δ 12.11 (d, *J* = 13.7 Hz, 1H), 10.66 (d, *J* = 12.8 Hz, 1H), 10.32 (d, *J* = 14.0 Hz, 1H), 8.60 (s, 1H), 8.50–8.30 (m, 2H), 8.22 (d, *J* = 14.8 Hz, 1H), 7.83 (dd, *J* = 51.5, 10.7 Hz, 5H), 7.34–7.00 (m, 3H), 6.75 (d, *J* = 12.8 Hz, 1H), 3.76 (d, *J* = 14.8 Hz, 3H), 3.57 (s, 2H), 2.96 (s, 2H), 2.36 (d, *J* = 14.4 Hz, 3H). ^{13}C NMR (100 MHz, DMSO-d_6, δ, ppm) δ 176.25, 165.62, 152.99, 150.46, 149.34, 143.64, 141.43, 136.90, 134.06, 131.34, 127.65, 127.08, 124.86, 123.28, 120.22, 112.00, 111.79, 111.05, 100.19, 55.30, 25.20, 17.93. HR-MS (ESI), calcd. $C_{26}H_{26}N_6O_2S$, $[M+H]^+m/z$: 487.1916. Found: 487.1908.

*4.4.12. (E)-N-(2-(2-methyl-1H-indol-3-yl)ethyl)-4-(2-((5-methylpyridin-2-yl)methylene)hydrazine-1-carbothioamido)benzamide (**16f**)*

White solid, m. p. 199.1–202.4 °C, yield 48%, purity 99.07%. ^{1}H NMR (400 MHz, DMSO-d_6, ppm) δ 12.09 (s, 1H), 10.71 (s, 1H), 10.31 (s, 1H), 8.59 (t, *J* = 5.6 Hz, 1H), 8.44 (s, 1H), 8.35 (d, *J* = 8.1 Hz, 1H), 8.20 (s, 1H), 7.92–7.80 (m, 2H), 7.71 (dd, *J* = 12.4, 8.7 Hz, 3H), 7.50 (d, *J* = 7.7 Hz, 1H), 7.24 (d, *J* = 7.8 Hz, 1H), 6.96 (dt, *J* = 14.6, 7.0 Hz, 2H), 3.46–3.40 (m, 2H), 2.91 (t, *J* = 7.3 Hz, 2H), 2.33 (d, *J* = 4.7 Hz, 6H). ^{13}C NMR (100 MHz, DMSO-d_6, δ, ppm) δ 175.94, 165.61, 150.46, 149.58, 143.61, 141.37, 136.91, 135.21, 134.06, 132.07, 131.32, 128.37, 127.04, 124.85, 120.21, 119.89, 118.07, 117.31, 110.35, 107.69, 24.11, 17.93, 11.19. HR-MS (ESI), calcd. $C_{26}H_{26}N_6OS$, $[M+H]^+m/z$: 471.1967. Found: 471.1969.

*4.4.13. (E)-N-(2-(5-methoxy-1H-indol-3-yl)ethyl)-4-(2-(pyridin-2-ylmethylene)hydrazine-1-carbothioamido)benzamide (**16g**)*

Yellow solid, m. p. 188.1–188.5 °C, yield 56%, purity 98.32%. ^{1}H NMR (400 MHz, DMSO-d_6, ppm) δ 12.14 (s, 1H), 10.66 (d, *J* = 13.4 Hz, 1H), 10.35 (s, 1H), 8.60 (d, *J* = 3.6 Hz, 2H), 8.45 (d, *J* = 8.0 Hz, 1H), 8.23 (s, 1H), 7.87 (t, *J* = 7.3 Hz, 3H), 7.73 (d, *J* = 8.4 Hz, 2H), 7.46–7.34 (m, 1H), 7.24 (d, *J* = 8.7 Hz, 1H), 7.16 (s, 1H), 7.08 (s, 1H), 6.81–6.66 (m, 1H), 3.74 (s, 3H), 3.56 (dd, *J* = 12.8, 6.7 Hz, 2H), 2.94 (t, *J* = 7.2 Hz, 2H). ^{13}C NMR (100 MHz, DMSO-d_6, δ, ppm) δ 176.12, 165.62, 153.00, 149.37, 143.47, 141.37, 136.49, 131.37, 127.63, 127.09, 124.90, 124.32, 123.28, 120.67, 111.98, 111.77, 111.06, 100.18, 55.30, 25.19. HR-MS (ESI), calcd. $C_{25}H_{24}N_6O_2S$, $[M+H]^+m/z$: 473.1760. Found: 473.1762.

*4.4.14. (E)-4-(2-((5-hydroxypyridin-2-yl)methylene)hydrazine-1-carbothioamido)-N-(2-(5-methoxy-1H-indol-3-yl)ethyl)benzamide (**16h**)*

White solid, m. p. 210.1–213.4 °C, yield 51%, purity 96.94%. ^{1}H NMR (400 MHz, DMSO-d_6, ppm) δ 11.97 (s, 1H), 10.64 (s, 1H), 10.37 (s, 1H), 10.22 (s, 1H), 8.58 (t, J = 5.5 Hz, 1H), 8.30 (d, J = 8.7 Hz, 1H), 8.24–8.06 (m, 2H), 7.86 (d, J = 8.6 Hz, 2H), 7.75 (d, J = 8.6 Hz, 2H), 7.23 (d, J = 8.7 Hz, 2H), 7.15 (d, J = 1.7 Hz, 1H), 7.08 (d, J = 2.1 Hz, 1H), 6.72 (dd, J = 8.7, 2.2 Hz, 1H), 3.74 (s, 3H), 3.55 (dd, J = 13.0, 7.1 Hz, 2H), 2.94 (t, J = 7.3 Hz, 2H). ^{13}C NMR (100 MHz, DMSO-d_6, δ, ppm) δ 175.58, 165.63, 154.66, 152.97, 144.13, 143.86, 141.47, 137.43, 131.37, 131.14, 127.63, 127.06, 124.58, 123.27, 122.64, 121.90, 111.97, 111.78, 111.06, 100.18, 55.30, 25.20. HR-MS (ESI), calcd. $C_{25}H_{24}N_6O_3S$, $[M+H]^+m/z$: 489.1709. Found: 489.1701.

*4.4.15. (E)-N-(2-(5-methoxy-1H-indol-3-yl)ethyl)-4-(2-((5-methoxypyridin-2-yl)methylene)hydrazine-1-carbothioamido)benzamide (**16i**)*

White solid, m. p. 204.5–206.7 °C, yield 46%, purity 99.27%. ^{1}H NMR (400 MHz, DMSO-d_6, ppm) δ 12.02 (s, 1H), 10.64 (s, 1H), 10.28 (s, 1H), 8.59 (t, J = 5.6 Hz, 1H), 8.41 (d, J = 8.8 Hz, 1H), 8.31 (d, J = 2.7 Hz, 1H), 8.20 (s, 1H), 7.87 (d, J = 8.6 Hz, 2H), 7.73 (d, J = 8.6 Hz, 2H), 7.53–7.42 (m, 1H), 7.23 (d, J = 8.7 Hz, 1H), 7.15 (d, J = 2.2 Hz, 1H), 7.08 (d, J = 2.3 Hz, 1H), 6.72 (dd, J = 8.7, 2.4 Hz, 1H), 3.89 (s, 3H), 3.74 (s, 3H), 3.55 (dd, J = 13.2, 7.2 Hz, 2H), 2.94 (t, J = 7.4 Hz, 2H). ^{13}C NMR (100 MHz, DMSO-d_6, δ, ppm) δ 175.76, 165.64, 156.07, 152.97, 145.52, 143.43, 141.45, 136.72, 131.37, 131.23, 127.62, 127.07, 124.77, 123.27, 121.70, 121.23, 111.98, 111.77, 111.05, 100.18, 55.82, 55.30, 25.19. HR-MS (ESI), calcd. $C_{26}H_{26}N_6O_3S$, $[M+H]^+m/z$: 503.1865. Found: 503.1857.

*4.4.16. (E)-N-(2-(2-methyl-1H-indol-3-yl)ethyl)-4-(2-(pyridin-2-ylmethylene)hydrazine-1-carbothioamido)benzamide (**16j**)*

White solid, m. p. 196.4–198.1 °C, yield 60%, purity 98.97%. ^{1}H NMR (400 MHz, DMSO-d_6, ppm) δ 12.14 (s, 1H), 10.69 (d, J = 12.5 Hz, 1H), 10.34 (s, 1H), 8.59 (t, J = 6.0 Hz, 2H), 8.45 (d, J = 8.0 Hz, 1H), 8.23 (s, 1H), 7.87 (t, J = 7.8 Hz, 3H), 7.73 (d, J = 8.5 Hz, 2H), 7.50 (d, J = 7.5 Hz, 1H), 7.41 (dd, J = 6.7, 5.4 Hz, 1H), 7.24 (d, J = 7.8 Hz, 1H), 6.96 (dt, J = 14.5, 6.9 Hz, 2H), 3.43 (dd, J = 13.3, 6.5 Hz, 2H), 2.91 (t, J = 7.4 Hz, 2H), 2.33 (s, 3H). ^{13}C NMR (100 MHz, DMSO-d_6, δ, ppm) δ 176.08, 165.60, 153.04, 149.37, 143.46, 141.33, 136.49, 135.21, 132.07, 131.38, 128.37, 127.06, 124.89, 124.32, 120.67, 119.89, 118.07, 117.31, 110.35, 107.69, 24.12, 11.19. HR-MS (ESI), calcd. $C_{25}H_{24}N_6OS$, $[M+H]^+m/z$: 457.1811. Found: 457.1813.

*4.4.17. (E)-4-(2-((5-hydroxypyridin-2-yl)methylene)hydrazine-1-carbothioamido)-N-(2-(2-methyl-1H-indol-3-yl)ethyl)benzamide (**16k**)*

Yellow solid, m. p. 218.5–219.4 °C, yield 51%, purity 98.66%. ^{1}H NMR (400 MHz, DMSO-d_6, ppm) δ 11.98 (s, 1H), 10.73 (s, 1H), 10.54 (s, 1H), 10.22 (s, 1H), 8.60 (t, J = 5.5 Hz, 1H, 8.30 (d, J = 8.7 Hz, 1H), 8.17 (s, 2H), 7.84 (t, J = 8.5 Hz, 2H), 7.81–7.70 (m, 2H), 7.50 (d, J = 7.5 Hz, 1H), 7.25 (dd, J = 9.5, 4.6 Hz, 2H), 6.96 (dt, J = 14.6, 7.0 Hz, 2H), 3.43 (d, J = 6.4 Hz, 2H), 2.91 (t, J = 7.2 Hz, 2H), 2.33 (s, 3H). ^{13}C NMR (100 MHz, DMSO-d_6, δ, ppm) δ 175.53, 165.61, 154.75, 144.06, 143.88, 141.43, 137.46, 135.21, 131.74, 131.13, 128.37, 127.03, 124.57, 122.64, 121.87, 119.88, 118.06, 117.31, 110.35, 107.69, 24.12, 11.19. HR-MS (ESI), calcd. $C_{25}H_{24}N_6O_2S$, $[M+H]^+m/z$: 473.1760. Found: 473.1762.

*4.4.18. (E)-4-(2-((5-methoxypyridin-2-yl)methylene)hydrazine-1-carbothioamido)-N-(2-(2-methyl-1H-indol-3-yl)ethyl)benzamide (**16l**)*

Red solid, m. p. 207.7–208.6 °C, yield 55%, purity 98.40%. ^{1}H NMR (400 MHz, DMSO-d_6, ppm) δ 12.02 (s, 1H), 10.71 (s, 1H), 10.27 (s, 1H), 8.58 (s, 1H), 8.41 (d, J = 8.8 Hz, 1H), 8.31 (s, 1H), 8.20 (s, 1H), 7.84 (t, J = 8.7 Hz, 2H), 7.73 (d, J = 7.7 Hz, 2H), 7.48 (t, J = 8.0 Hz, 2H), 7.23 (d, J = 7.7 Hz, 1H), 7.07–6.84 (m, 2H), 3.89 (s, 3H), 3.42 (d, J = 6.1 Hz, 2H, 2.90 (t, J = 6.9 Hz, 2H), 2.33 (s, 3H). ^{13}C NMR (100 MHz, DMSO-d_6, δ, ppm) δ 175.73, 165.60, 156.07, 145.54, 143.43, 141.41, 136.70, 135.21, 132.06, 131.25, 128.37, 127.03, 124.79, 121.66, 121.23, 119.89, 118.07, 117.31, 110.35, 107.70, 55.82, 24.12, 11.19. HR-MS (ESI), calcd. $C_{26}H_{26}N_6O_2S$, $[M+H]^+m/z$: 487.1916. Found: 487.1915.

*4.4.19. (E)-6-((2-((4-((2-(2-methyl-1H-indol-3-yl)ethyl)carbamoyl)phenyl)carbamothioyl)hydrazono)methyl)nicotinate (**16 m**)*

Yellow solid, m. p. 205.4–206.1 °C, yield 51%, purity 98.46%. ^{1}H NMR (400 MHz, DMSO-d_6, ppm) δ 12.29 (s, 1H), 10.71 (s, 1H), 10.47 (s, 1H), 9.09 (s, 1H), 8.60 (d, J = 7.8 Hz, 2H), 8.37–8.19 (m, 2H), 7.87 (d, J = 8.4 Hz, 2H), 7.71 (d, J = 8.4 Hz, 2H), 7.50 (d, J = 7.3 Hz, 1H), 7.24 (d, J = 7.7 Hz, 1H), 6.96 (d t, J = 14.5, 6.8 Hz, 2H), 3.91 (s, 3H), 3.43 (d, J = 5.6 Hz, 2H), 2.91 (t, J = 7.2 Hz, 2H), 2.29 (d, J = 31.1 Hz, 3H). ^{13}C NMR (100 MHz, DMSO-d_6, δ, ppm) δ 176.34, 165.58, 164.98, 156.81, 149.97, 142.01, 141.25, 136.93, 135.20, 132.07, 131.57, 128.36, 127.10, 125.21, 125.14, 120.36, 119.89, 118.07, 117.31, 110.35, 107.68, 52.46, 40.37, 24.11, 11.19. HR-MS (ESI), calcd. $C_{27}H_{26}N_6O_3S$, $[M+H]^+m/z$: 515.1865. Found: 515.1858.

*4.4.20. (E)-4-(2-((5-bromopyridin-2-yl)methylene)hydrazine-1-carbothioamido)-N-(2-(2-methyl-1H-indol-3-yl)ethyl)benzamide (**16n**)*

White solid, m. p. 201.2–203.8 °C, yield 54%, purity 97.93%. ^{1}H NMR (400 MHz, DMSO-d_6, ppm) δ 12.20 (s, 1H), 10.72 (s, 1H), 10.41 (s, 1H), 8.73 (s, 1H), 8.61 (s, 1H), 8.46 (d, J = 8.6 Hz, 1H), 8.26–8.10 (m, 2H), 7.86 (d, J = 8.3 Hz, 2H), 7.70 (d, J = 8.3 Hz, 2H), 7.49 (d, J = 7.4 Hz, 1H), 7.24 (d, J = 7.8 Hz, 1H), 6.96 (dt, J = 14.6, 7.0 Hz, 2H), 3.42 (d, J = 6.0 Hz, 2H), 2.90 (t, J = 7.0 Hz, 2H), 2.33 (s, 3H). ^{13}C NMR (100 MHz, DMSO-d_6, δ, ppm) δ 176.15, 165.57, 151.92, 150.07, 142.17, 141.28, 139.18, 135.19, 132.06, 131.48, 128.36, 127.08, 125.11, 122.23, 120.81, 119.89, 118.07, 117.31, 110.35, 107.68, 40.37, 24.11, 11.19. HR-MS (ESI), calcd. $C_{25}H_{23}BrN_6OS$, $[M+H]^+m/z$: 535.0915. Found: 535.0908.

*4.4.21. (E)-4-(2-((5-chloropyridin-2-yl)methylene)hydrazine-1-carbothioamido)-N-(2-(2-methyl-1H-indol-3-yl)ethyl)benzamide (**16o**)*

Yellow solid, m. p. 205.2–206.8 °C, yield 52%, purity 97.21%. White solid, m. p. 205.2–203.8 °C, yield 52%. ^{1}H NMR (400 MHz, DMSO-d_6, ppm) δ 12.19 (s, 1H), 10.72 (s, 1H), 10.41 (s, 1H), 8.63 (d, J = 17.4 Hz, 2H), 8.53 (d, J = 8.6 Hz, 1H), 8.20 (s, 1H), 8.03 (d, J = 8.5 Hz, 1H), 7.86 (d, J = 8.4 Hz, 2H), 7.70 (d, J = 8.3 Hz, 2H), 7.50 (d, J = 7.5 Hz, 1H), 7.24 (d, J = 7.7 Hz, 1H), 6.96 (dt, J = 14.8, 7.0 Hz, 2H), 3.43 (d, J = 6.2 Hz, 2H), 2.91 (t, J = 7.1 Hz, 2H), 2.33 (s, 3H). ^{13}C NMR (100 MHz, DMSO-d_6, δ, ppm) δ 176.15, 165.57, 151.70, 147.90, 142.06, 141.28, 136.43, 135.20, 132.06, 131.46, 128.36, 127.08, 125.09, 121.85, 119.89, 118.07, 117.52, 110.35, 107.68, 40.37, 24.11, 11.19. HR-MS (ESI), calcd. $C_{25}H_{23}ClN_6OS$, $[M+H]^+m/z$: 491.1421. Found: 491.1413.

*4.4.22. (E)-N-(2-(2-methyl-1H-indol-3-yl)ethyl)-4-(2-(1-(pyridin-2-yl)ethylidene)hydrazine-1-carbothioamido)benzamide (**16p**)*

Yellow solid, m. p. 198.2–199.5 °C, yield 54%, purity 98.44%. ^{1}H NMR (400 MHz, DMSO-d_6, ppm) δ 10.81 (s, 1H), 10.70 (s, 1H), 10.27 (s, 1H), 8.56 (dd, J = 25.4, 10.0 Hz, 3H), 7.85 (d, J = 8.1 Hz, 3H), 7.73 (d, J = 8.1 Hz, 2H), 7.49 (d, J = 7.6 Hz, 1H), 7.45–7.35 (m, 1H), 7.23 (d, J = 7.8 Hz, 1H), 7.03–6.79 (m, 2H), 3.42 (d, J = 5.9 Hz, 2H), 2.91 (d, J = 7.1 Hz, 2H), 2.49 (s, 3H), 2.32 (s, 3H). ^{13}C NMR (100 MHz, DMSO-d_6, δ, ppm) δ 176.93, 165.59, 154.43, 149.66, 148.49, 141.49,

136.40, 135.22, 132.07, 131.38, 128.38, 127.05, 124.94, 124.17, 121.27, 119.89, 118.07, 117.31, 110.35, 107.70, 40.37, 24.12, 12.59, 11.19. HR-MS (ESI), calcd. $C_{26}H_{26}N_6OS$, $[M+H]^+m/z$: 471.1967. Found: 471.1959.

4.4.23. (E)-N-(2-(5-methoxy-1H-indol-3-yl)ethyl)-4-(2-(1-(pyridin-2-yl)ethylidene)hydrazine-1-carbothioamido)benzamide (**16q**)

White solid, m. p. 201.1–203.5 °C, yield 48%, purity 98.50%. ^{1}H NMR (400 MHz, DMSO-d_6, ppm) δ 10.80 (s, 1H), 10.64 (s, 1H), 10.28 (s, 1H), 8.60 (d, J = 10.0 Hz, 2H), 8.53 (d, J = 8.2 Hz, 1H), 7.85 (dd, J = 15.8, 8.1 Hz, 3H), 7.73 (d, J = 8.1 Hz, 2H), 7.46–7.37 (m, 1H), 7.23 (d, J = 8.7 Hz, 1H), 7.15 (s, 1H), 7.07 (s, 1H), 6.72 (d, J = 8.6 Hz, 1H), 3.74 (s, 3H), 3.55 (d, J = 6.1 Hz, 2H), 2.94 (t, J = 7.0 Hz, 2H), 2.49 (s, 3H). ^{13}C NMR (100 MHz, DMSO-d_6, δ, ppm) δ 176.96, 165.61, 154.44, 152.98, 149.69, 148.50, 141.53, 136.40, 131.37, 127.63, 127.08, 124.94, 124.17, 123.27, 121.27, 111.97, 111.77, 111.05, 100.19, 55.31, 40.22, 25.20, 12.60. HR-MS (ESI), calcd. $C_{26}H_{26}N_6O_2S$, $[M+H]^+m/z$: 487.1916. Found: 487.1908.

4.4.24. (E)-4-(2-(2-hydroxybenzylidene)hydrazine-1-carbothioamido)-N-(2-(2-methyl-1H-indol-3-yl)ethyl)benzamide (**16r**)

Yellow solid, m. p. 204.1–206.4 °C, yield 38%, purity 97.13%. ^{1}H NMR (400 MHz, DMSO-d_6, ppm) δ 11.89 (s, 1H), 10.71 (s, 1H), 10.16 (s, 1H), 10.00 (s, 1H), 8.55 (d, J = 21.7 Hz, 2H), 8.10 (d, J = 6.7 Hz, 1H), 7.79 (dd, J = 34.3, 8.3 Hz, 4H), 7.49 (d, J = 7.4 Hz, 1H), 7.25 (t, J = 9.3 Hz, 2H), 7.06–6.77 (m, 4H), 3.42 (d, J = 6.3 Hz, 2H), 2.90 (t, J = 7.0 Hz, 2H), 2.32 (s, 3H). ^{13}C NMR (100 MHz, DMSO-d_6, δ, ppm) δ 165.62, 156.66, 141.55, 135.20, 132.06, 131.44, 130.95, 128.36, 126.99, 124.40, 120.14, 119.89, 119.21, 118.07, 117.31, 116.03, 110.35, 107.69, 40.36, 24.12, 11.19. HR-MS (ESI), calcd. $C_{26}H_{25}N_5O_2S$, $[M+H]^+m/z$: 472.1807. Found: 472.1799.

4.4.25. (E)-N-(2-(2-methyl-1H-indol-3-yl)ethyl)-4-(2-(2-oxoindolin-3-ylidene)hydrazine-1-carbothioamido)benzamide (**16s**)

White solid, m. p. 207.1.2–208.7 °C, yield 35%, purity 96.32%. ^{1}H NMR (400 MHz, DMSO-d_6, ppm) δ 12.87 (s, 1H), 11.28 (s, 1H), 10.91 (s, 1H), 10.72 (s, 1H), 8.63 (s, 1H), 7.89 (d, J = 8.5 Hz, 2H), 7.79 (t, J = 8.2 Hz, 3H), 7.51 (t, J = 14.0 Hz, 1H), 7.39 (t, J = 7.6 Hz, 1H), 7.23 (d, J = 7.7 Hz, 1H), 7.12 (dd, J = 15.1, 7.7 Hz, 1H), 7.07–6.89 (m, 3H), 3.43 (d, J = 6.6 Hz, 2H), 2.91 (t, J = 7.4 Hz, 2H), 2.33 (s, 3H). ^{13}C NMR (100 MHz, DMSO-d_6, δ, ppm) δ 176.08, 165.50, 162.70, 142.57, 140.80, 135.20, 132.59, 132.07, 131.95, 131.55, 128.36, 127.31, 124.63, 122.37, 121.46, 119.89, 119.82, 118.07, 117.30, 111.12, 110.35, 107.67, 40.38, 24.09, 11.19. HR-MS (ESI), calcd. $C_{27}H_{24}N_6O_2S$, $[M+H]^+m/z$: 497.1759. Found: 497.1752.

4.5. General procedure for the synthesis of compound(22)

Intermediate **20** was synthesized from commercially available **17**, according to our previously reported methods [39]. To a solution of **20** (5 mmol) in H_2O (50 mL) was added sodium hydroxide (15 mmol) dropwise. The reaction was heated to 80 °C for 4 h and then cooled to room temperature. After the mixture was acidified with 1 M HCl, the precipitated product was filtered off and washed with H_2O to give **21** as white solid. In a 25 mL round-bottom flask, intermediate **21** (0.5 mmol), 2-(1H-indol-3-yl) ethan-1-amine (0.5 mmol), EDCI (0.5 mmol) and HOBT (0.5 mmol) were dissolved in dichloromethane (12 mL) and stirred at room temperature for 6 h. Upon completion, H_2O was added. The aqueous layer was extracted twice with dichloromethane. The collective organic layers were evacuated to provide the residue, which was then purified by chromatography (silica gel, 10% methanol/dichloromethane) to give compound **22** as a white solid in 46% yields.

4.5.1. (E)-4-((2-((5-methylpyridin-2-yl)methylene)hydrazine-1-carbothioamido)methyl)benzoic acid (**21**)

Yellow solid, m. p. 154.4–155.1 °C, yield 41%. ^{1}H NMR (400 MHz, DMSO-d_6, ppm) δ 12.84 (s, 1H), 11.82 (s, 1H), 9.28 (s, 1H), 8.42 (s, 1H), 8.29–8.02 (m, 2H), 7.92 (d, J = 8.0 Hz, 2H), 7.67 (d, J = 8.0 Hz, 1H), 7.45 (d, J = 7.9 Hz, 2H), 4.92 (d, J = 5.7 Hz, 2H), 3.18 (s, 2H), 2.32 (s, 3H). ^{13}C NMR (100 MHz, DMSO-d_6, δ, ppm) δ 177.95, 167.19, 150.60, 149.43, 144.50, 142.65, 136.97, 133.82, 129.28, 129.20, 127.10, 119.81, 48.57, 46.47, 17.88. HR-MS (ESI), calcd. $C_{16}H_{16}N_4O_2S$ $[M+H]^+m/z$: 329.1072. Found: 329.1065.

4.5.2. (E)-N-(2-(1H-indol-3-yl)ethyl)-4-((2-((5-methylpyridin-2-yl)methylene)hydrazine-1-carbothioamido)methyl)benzamide (**22**)

White solid, m. p. 200.1–202.5 °C, yield 46%, purity 99.00%. ^{1}H NMR (400 MHz, DMSO-d_6, ppm) δ 11.81 (s, 1H), 10.80 (s, 1H), 9.26 (s, 1H), 8.56 (s, 1H), 8.42 (s, 1H), 8.20 (d, J = 8.1 Hz, 1H), 8.13 (s, 1H), 7.82 (d, J = 7.8 Hz, 2H), 7.66 (d, J = 8.0 Hz, 1H), 7.59 (d, J = 7.7 Hz, 1H), 7.41 (d, J = 7.8 Hz, 2H), 7.34 (d, J = 8.0 Hz, 1H), 7.17 (s, 1H), 7.07 (t, J = 7.4 Hz, 1H), 6.98 (t, J = 7.3 Hz, 1H), 4.90 (d, J = 5.5 Hz, 2H), 3.54 (d, J = 5.9 Hz, 2H), 2.95 (t, J = 7.1 Hz, 2H), 2.32 (s, 3H). ^{13}C NMR (100 MHz, DMSO-d_6, δ, ppm) δ 177.89, 165.93, 150.70, 149.53, 142.74, 142.42, 136.86, 136.21, 133.77, 133.22, 127.25, 127.06, 126.85, 122.58, 120.88, 119.74, 118.27, 118.19, 111.88, 111.34, 46.41, 25.19, 17.89. HR-MS (ESI), calcd. $C_{26}H_{26}N_6OS$, $[M+H]^+m/z$: 471.1967. Found: 471.1959.

4.6. General procedure for the synthesis of compound(25)

Following a similar procedure as compound **6**, compound **24** was obtained as a white solid. To a solution of **24** (2.4 mmol) and sodium hydroxide in THF/MeOH (1:1, 16 mL total) was added hydroxylamine solution dropwise. The resulting solution was stirred 30 min at room temperature. Upon completion, the reaction was quenched with acetic acid and concentrated in vacuo. The crude product was purified *via* flash chromatography on silica gel (10% methanol/dichloromethane) to afford the title analogue **25** as a white solid in 56% yields.

4.6.1. Methyl 4-((2-(2-methyl-1H-indol-3-yl)ethyl)carbamoyl) benzoate (**24**)

Yellow solid, m. p. 161.1–162.4 °C, yield 48%. ^{1}H NMR (400 MHz, DMSO-d_6, ppm) δ 10.72 (s, 1H), 8.80 (s, 1H), 8.03 (d, J = 8.1 Hz, 2H), 7.95 (d, J = 8.1 Hz, 2H), 7.47 (d, J = 7.5 Hz, 1H), 7.23 (d, J = 7.7 Hz, 1H), 6.95 (dt, J = 20.5, 7.1 Hz, 2H), 3.88 (s, 3H), 3.42 (d, J = 6.3 Hz, 2H), 2.90 (t, J = 7.2 Hz, 2H), 2.31 (s, 3H). ^{13}C NMR (100 MHz, DMSO-d_6, δ, ppm) δ 165.72, 165.22, 138.80, 135.20, 132.08, 131.60, 129.08, 128.34, 127.47, 119.89, 118.07, 117.26, 110.35, 107.55, 52.30, 40.44, 23.94, 11.15. HR-MS (ESI), calcd. $C_{20}H_{20}N_2O_3$, $[M+H]^+m/z$: 337.1552. Found: 337.1545.

4.6.2. N^1-hydroxy-N^4-(2-(2-methyl-1H-indol-3-yl)ethyl) terephthalamide (**25**)

White solid, m. p. 210.2–212.7 °C, yield 56%, purity 98.36%. ^{1}H NMR (400 MHz, DMSO-d_6, ppm) δ 10.74 (s, 1H), 9.15 (s, 1H), 8.66 (s, 1H), 7.89–7.67 (m, 4H), 7.48 (d, J = 7.5 Hz, 1H), 7.23 (d, J = 7.7 Hz, 1H), 6.95 (dt, J = 14.2, 6.9 Hz, 2H), 3.41 (d, J = 6.2 Hz, 3H), 2.89 (t, J = 7.2 Hz, 2H), 2.31 (s, 3H). ^{13}C NMR (100 MHz, DMSO-d_6, δ, ppm) δ 165.66, 135.20, 132.07, 128.34, 126.82, 126.26, 119.87, 118.05, 117.29, 110.35, 107.62, 40.36, 24.03, 11.17. HR-MS (ESI), calcd. $C_{19}H_{19}N_3O_3$, $[M+H]^+m/z$: 338.1504. Found: 338.1497.

4.7. General procedure for the synthesis of compound(28)

6-hydrazinylnicotinic acid **26** (2 mmol) was dissolved in ethanol (15 mL), and 2-acetylpyridine (2 mmol) was added followed by the addition of catalytic amount acetic acid (0.2 mmol). Stirring was continued for 5 h at 80°*C* until TLC displayed consumption of starting material. The precipitated solid was filtered off and washed with ethanol to provide the crude product, which was recrystallized from ethanol to give the pure **27**. Compound **27** (1.2 mmol) was dissolved in dichloromethane followed by the addition of 2-(2-methyl-1H-indol-3-yl) ethan-1-amine (1.2 mmol), EDCI (1.2 mmol) and HOBT (1.2 mmol). Stirring was continued at room temperature until TLC displayed consumption of starting materials. Then, solvent was removed, followed by addition of water and dichloromethane. Afterwards, the phases were separated, the organic phase was dried, and concentrated in vacuo. The crude product was purified *via* flash chromatography on silica gel (10% methanol/dichloromethane) to give the derivative **28** as a white solid in 50% yield.

4.7.1. (E)-4-(2-(1-(pyridin-2-yl)ethylidene)hydrazinyl)benzoic acid (**27**)

White solid, m. p. 170.1–172.3 °C, yield 53%. ^{1}H NMR (400 MHz, DMSO-d_6, ppm) δ 12.74 (s, 1H), 10.58 (s, 1H), 8.73 (s, 1H), 8.58 (d, J = 3.7 Hz, 1H), 8.15 (dd, J = 13.2, 8.6 Hz, 2H), 7.83 (t, J = 7.6 Hz, 1H), 7.52–7.29 (m, 2H), 2.43 (s, 3H). ^{13}C NMR (100 MHz, DMSO-d_6, δ, ppm) δ 166.40, 159.75, 155.40, 150.17, 148.47, 146.94, 138.92, 136.39, 123.27, 119.78, 118.07, 106.39, 11.64. HR-MS (ESI), calcd. $C_{14}H_{13}N_3O_2$, $[M+H]^+m/z$: 257.1038. Found: 257.1033.

4.7.2. (E)-N-(2-(2-methyl-1H-indol-3-yl)ethyl)-6-(2-(1-(pyridin-2-yl)ethylidene)hydrazinyl)nicotinamide (**28**)

White solid, m. p. 205.2–207.1 °C, yield 50%, purity 98.36%. ^{1}H NMR (400 MHz, DMSO-d_6, ppm) δ 10.73 (s, 1H), 10.41 (s, 1H), 8.67 (t, J = 10.1 Hz, 1H), 8.56 (dd, J = 11.5, 5.3 Hz, 2H), 8.19 (d, J = 8.1 Hz, 1H), 8.13 (dd, J = 8.8, 2.2 Hz, 1H), 7.82 (td, J = 8.0, 1.7 Hz, 1H), 7.54–7.29 (m, 3H), 7.24 (d, J = 7.7 Hz, 1H), 7.06–6.86 (m, 2H), 3.41 (dd, J = 13.7, 6.6 Hz, 2H), 2.90 (t, J = 7.4 Hz, 2H), 2.43 (s, 3H), 2.30 (d, J = 25.5 Hz, 3H). ^{13}C NMR (100 MHz, DMSO-d_6, δ, ppm) δ 165.16, 159.21, 156.04, 148.93, 148.13, 146.47, 137.51, 136.85, 135.70, 132.55, 128.88, 123.61, 122.48, 120.39, 120.24, 118.57, 117.81, 110.86, 108.21, 106.60, 40.72, 24.69, 12.01, 11.67. HR-MS (ESI), calcd. $C_{24}H_{24}N_6O$, $[M+H]^+m/z$: 413.2090. Found: 413.2090.

4.8. General procedure for the synthesis of compound(31)

Commercially available **23** and **10e** were converted to intermediate **29** *via* a similar reaction of Scheme 6b. Intermediate **29** (3.6 mmol) then was dissolved in methanol (15 mL) followed by the addition of hydrazine hydrate (36 mmol). Stirring was continued at 80 °C until TLC displayed consumption of starting material. The reaction mixture was cooled at room temperature and filtered to provide intermediate **30** as a white solid. Following a similar procedure as scheme 6a, compound **31** was obtained as a white solid in 41% yield.

4.8.1. 4-(hydrazinecarbonyl)-N-(2-(2-methyl-1H-indol-3-yl)ethyl) benzamide (**30**)

White solid, m. p. 172.1–173.4 °C, yield 65%. ^{1}H NMR (400 MHz, DMSO-d_6, ppm) δ 10.71 (s, 1H), 9.88 (s, 1H), 8.69 (s, 1H), 7.88 (s, 4H), 7.47 (d, J = 7.3 Hz, 1H), 7.23 (d, J = 7.7 Hz, 1H), 6.95 (dt, J = 14.5, 6.9 Hz, 2H), 4.58 (s, 2H), 3.42 (d, J = 5.8 Hz, 2H), 2.90 (t, J = 7.0 Hz, 2H), 2.31 (s, 3H). ^{13}C NMR (100 MHz, DMSO-d_6, δ, ppm) δ 165.42, 165.14, 136.83, 135.38, 135.19, 132.08, 128.34, 127.07, 126.87, 119.89, 118.07, 117.28, 110.35, 107.59, 40.40, 23.99, 11.17. HR-MS (ESI), calcd. $C_{19}H_{20}N_4O_2$, $[M+H]^+m/z$: 337.1664. Found: 337.1664.

4.8.2. (E)-4-(2-((3-hydroxy-5-(hydroxymethyl)-2-methylpyridin-4-yl)methylene)hydrazine-1-carbonyl)-N-(2-(2-methyl-1H-indol-3-yl)ethyl)benzamide (**31**)

White solid, m. p. 211.4.2–212.7 °C, yield 41%, purity 98.66%. ^{1}H NMR (400 MHz, DMSO-d_6, ppm) δ 13.34 (s, 1H), 13.18 (s, 1H), 10.75 (s, 1H), 9.13 (s, 1H), 8.85 (s, 1H), 8.29–7.88 (m, 5H), 7.49 (d, J = 7.5 Hz, 1H), 7.23 (d, J = 7.8 Hz, 1H), 6.96 (dt, J = 14.7, 7.1 Hz, 2H), 4.79 (s, 2H), 3.44 (d, J = 6.3 Hz, 2H), 2.92 (t, J = 7.1 Hz, 2H), 2.65 (s, 3H), 2.33 (s, 3H). ^{13}C NMR (100 MHz, DMSO-d_6, δ, ppm) δ 165.15, 162.56, 152.93, 144.06, 143.37, 138.26, 136.76, 135.19, 133.35, 132.10, 129.48, 128.34, 128.01, 127.43, 119.89, 118.06, 117.27, 110.36, 107.56, 58.08, 40.46, 23.97, 14.66, 11.18. HR-MS (ESI), calcd. $C_{27}H_{27}N_5O_4$, $[M+H]^+m/z$: 472.1985. Found: 472.1982.

4.9. Cell culture and reagents

Human esophageal cancer cell line (EC109), human gastric cancer cell line (MGC803), human breast cancer cell line (MCF-7), human prostatic cancer cell line (PC3, DU-145) and normal prostatic cell line (WPMY-1) were all initially purchased from the Cell Bank of Shanghai. They were cultured in RPMI-1640 or DMEM (Solarbio, China) complete medium (10% fetal bovine serum, 100 U/mL penicillin and 100 g/mL streptomycin antibiotics) in a 5% CO2 humidified atmosphere at 37°*C*. FBS was purchased from Bioind and medium was obtained from Solarbio. The synthetic compounds were placed at −20°*C* after dissolved in DMSO at a storage concentration of 20 mM. Hoechst 33,342, PI, RNase A and NAC were purchased from Solarbio. Reactive Oxygen Species Assay Kit and Annexin V-FITC/PI Apoptosis Detection Kit were bought from Beyotime Biotechnology.

4.10. assay

Cells were seeded in the 96-well plates at a concentration of 2–3 × 10^3 cells per well. Next day, 200 μL fresh complete medium with serial of concentrations of compounds were added to the plates and then were maintained for 24 h, 48 h and 72 h, respectively. PC3 cells were treated with IC_{50} concentrations of several analogues in the presence of 20 μM Fe^{3+} for 72 h. PC3 and DU-145 cells were pre-treated with 4 mM SB203580 for 4 h, followed by 72 h treatment with IC_{50} concentration of compound **16f**, respectively. After that, 20 μL MTT solution (5 mg/mL, dissolved in PBS) was added to per well. After incubation for another 4 h at 37°*C* in the dark, the plates were measured by a microplate reader at 490 nm. The absorbance value was analyzed, and IC_{50} was calculated by SPSS software.

4.11. Colony assay

Cells seeded into 6-well plates at a concentration of 1 × 10^3 cells per well were cultured overnight. Then cells were treated with indicated concentrations of compound **16f** for 6 days, respectively. Subsequently, after fixation in 4% paraformaldehyde for 1 h at 4 °*C*, cells were stained by 1% crystal violet dissolved in methyl alcohol for 30 min at room temperature and then photographed. After that, crystal violet was dissolved in 75% ethyl alcohol and measured using a microplate reader at 595 nm.

4.12. Cell cycle assay

Cells were treated with indicated concentrations of compound

16f in 6-well plates for 48 h. Then they were harvested and washed in PBS. After fixation in 1 mL 70% ethyl alcohol at 4°*C* for more than 24 h, cells were incubated in PI staining buffer containing 1 mg/mL PI and 10 mg/mL RNase A for another 30 min at room temperature in the dark. Subsequently, cells were diluted in PBS, filtered by 200-mesh nylon mesh and then analyzed using flow cytometry.

4.13. Hoechst 33,342 staining

Cells seeded in 24-well plates were treated with compound 16f at indicated concentrations for 72 h. After fixation in 4% paraformaldehyde for 1 h at 4 °*C*, cells were cultured in 200 μL Hoechst 33,342 solution for 30 min at 37 °C in the dark and then photographed under fluorescence microscope.

4.14. Cell apoptosis assay

Cells seeded in 60-mm culture dish were treated with different concentrations of compound 16f for 72 h, respectively. After harvested and washed in PBS, cells were incubated in 200 μL binging buffer containing 2 μl Annexin V-FITC and 2 μl PI at room temperature for 10 min away from light. Next, another 800 μL PBS was added to the cells. Finally, cells were suspended, filtered and analyzed by flow cytometry.

4.15. ROS assay

Cells seeded in 6-well plates were cultured in fresh complete medium with indicated concentrations of 16f for 48 h, respectively. After harvested and washed, cells were incubated in medium with 10 μM DCFH-DA for 20 min at 37°*C* away from light. Then cells were washed in medium thrice and analyzed by flow cytometry.

4.16. Western blot analysis

Cells seeded in the 100-mm culture dish were treated with indicated concentrations of compound 16f for 48 h and 72 h, respectively. After harvested and washed in PBS, cells were suspended in RIPA lysis buffer with complete protease inhibitor on ice for 30 min. Next, protein lysis buffer was centrifuged for 15 min at 4 °C, and then supernatant was collected and quantified by BCA Protein Assay Kit. Subsequently, all protein samples were separated using 8%–12% SDS-PAGE gels and transferred to 0.22 μm nitrocellulose membranes. After blocking in 5% defatted milk at room temperature for 2 h, membranes were incubated with indicated primary antibodies (Bax, #5023; Bcl-2, #15071; P53, #2524; P27, #3686; Cleaved-Caspase 9, #7237; Cleaved-Caspase 3, #9661; Cleaved-PARP, #5625; p-ERK1/2, #8544; ERK1/2, #4695; p-JNK, #4668; JNK, #9252; p-P38, #4511; P38, #8690. They were all purchased from Cell Signaling Technology; GAPDH, TA-08, purchased from ZSGB-BIO) at 4 °C overnight. The second day, membranes was washed in PBST thrice and then were incubated with corresponding second antibodies (ZB-2301, ZB-2305, purchased from ZSGB-BIO) at room temperature for 2 h. Subsequently, ECL substrate was added to the surface of the membranes, and then the chemiluminescent signals were observed and collected by photographic film in the dark. Finally, the protein bands were analyzed using Image software.

4.17. Acute toxicity assay

8-12-week-old C57BL/6 wild mice were randomly divided into two groups: Con group and 16f treatment group (n = 10 per group). The mice were starved 12 h in advance. Compound 16f was dissolved in oil and given intragastrically at a dosage of 2 mg/kg, whereas the mice in the control group were given equal oil without compound. After that, the mice were fed normally and observed for 2 weeks. Finally, the major organs, heart, liver, spleen, lung, and kidney were harvested.

4.18. Hematoxylin and eosin (H&E) staining

The fresh tissues removed from mice were fixed in 4% paraformaldehyde for 48 h and then were embedded in paraffin. 5 μm sections were prepared and deparaffinized in xylene twice, rehydrated respectively in 100%, 95%, 80% and 70% ethanol. Afterwards, sections were stained with hematoxylin and eosin. Images were captured by high volume, digital whole slide scanning (Leica Biosystems).

4.19. In vivo antitumor activity

PC3 cells were prepared and then were subcutaneously implanted into the right flanks of the BALB/C-NU mice at a concentration of 1×10^7. When the tumor volume reached 100 mm^3, the mice were randomly divided into four groups: corresponding solvent (0.5% CMC-Na, negative control) group, 3-AP (10 mg/kg, positive control) group, 16f (12.5 mg/kg) treatment group, and 16f (25 mg/kg) treatment group. The 3-AP was subcutaneous injection every three days, while the solvent and treatment group mice received intragastric administration of equal solvent and 16f per day for 21 days. The body weight and tumor volume of these mice were measured every two days. Finally, the mice were euthanized, the body weight was measured and tumors were collected, weighed, and photographed.

Declaration of competing interest

The authors declare that they have no known competing financial interests or personal relationships that could have appeared to influence the work reported in this paper.

Acknowledgement

This work was supported by National Key Grant from Chinese Ministry of Science and Technology (2016YFA0501800 by Z. W), National Natural Science Foundation of China (NO. 81470524 and 81870297 by Z. W; NO. 81430085 by L.H-M; 81703328 by M. L-Y) and Henan Scientific Innovation Talent Team, Department of Education (19IRTSTHN001 by Z. W); the Starting Grant of Zhengzhou University (Grant 32210535 by M. L-Y); Scientific Program of Henan Province (Grant 182102310070 by M. L-Y).

Appendix A. Supplementary data

Supplementary data to this article can be found online at https://doi.org/10.1016/j.ejmech.2020.112970.

References

[1] Q. Yan, X. Chen, H. Gong, P. Qiu, X. Xiao, S. Dang, A. Hong, Y. Ma, Delivery of a TNF-alpha-derived peptide by nanoparticles enhances its antitumor activity by inducing cell-cycle arrest and caspase-dependent apoptosis, Faseb. J. 32 (2018) 6948–6964.

[2] S.G. Park, S.H. Kim, K.Y. Kim, S.N. Yu, H.D. Choi, Y.W. Kim, H.W. Nam, Y.K. Seo, S.C. Ahn, Toyocamycin induces apoptosis via the crosstalk between reactive oxygen species and p38/ERK MAPKs signaling pathway in human prostate cancer PC-3 cells, Pharmacol. Rep. 69 (2017) 90–96.

[3] W. Lim, M. Jeong, F.W. Bazer, G. Song, Coumestrol inhibits proliferation and migration of prostate cancer cells by regulating AKT, ERK1/2, and JNK MAPK cell signaling cascades, J. Cell. Physiol. 232 (2017) 862–871.

[4] V.F. Pape, S. Toth, A. Furedi, K. Szebenyi, A. Lovrics, P. Szabo, M. Wiese, G. Szakacs, Design, synthesis and biological evaluation of thiosemicarbazones, hydrazinobenzothiazoles and arylhydrazones as anticancer agents with a potential to overcome multidrug resistance, Eur. J. Med. Chem. 117 (2016) 335–354.
[5] Y. Yu, J. Wong, D.B. Lovejoy, D.S. Kalinowski, D.R. Richardson, Chelators at the cancer coalface: desferrioxamine to Triapine and beyond, Clin. Canc. Res. 12 (2006) 6876–6883.
[6] V.F. Pape, D. Turk, P. Szabo, M. Wiese, E.A. Enyedy, G. Szakacs, Synthesis and characterization of the anticancer and metal binding properties of novel pyrimidinylhydrazone derivatives, J. Inorg. Biochem. 144 (2015) 18–30.
[7] D.B. Lovejoy, P.J. Jansson, U.T. Brunk, J. Wong, P. Ponka, D.R. Richardson, Antitumor activity of metal-chelating compound Dp44mT is mediated by formation of a redox-active copper complex that accumulates in lysosomes, Canc. Res. 71 (2011) 5871–5880.
[8] C. Stefani, P.J. Jansson, E. Gutierrez, P.V. Bernhardt, D.R. Richardson, D.S. Kalinowski, Alkyl substituted 2'-benzoylpyridine thiosemicarbazone chelators with potent and selective anti-neoplastic activity: novel ligands that limit methemoglobin formation, J. Med. Chem. 56 (2013) 357–370.
[9] I. Machado, M. Fernández, L. Becco, B. Garat, R.F. Brissos, N. Zabarska, P. Gamez, F. Marques, I. Correia, J. Costa Pessoa, D. Gambino, New metal complexes of NNO tridentate ligands: effect of metal center and co-ligand on biological activity, Inorg. Chim. Acta. 420 (2014) 39–46.
[10] P. Heffeter, V.F.S. Pape, E.A. Enyedy, B.K. Keppler, G. Szakacs, C.R. Kowol, Anticancer thiosemicarbazones: chemical properties, interaction with iron metabolism, and resistance development, Antioxidants Redox Signal. 30 (2019) 1062–1082.
[11] N. Fortunati, F. Marano, A. Bandino, R. Frairia, M.G. Catalano, G. Boccuzzi, The pan-histone deacetylase inhibitor LBH589 (panobinostat) alters the invasive breast cancer cell phenotype, Int. J. Oncol. 44 (2014) 700–708.
[12] M. Carcelli, M. Tegoni, J. Bartoli, C. Marzano, G. Pelosi, M. Salvalaio, D. Rogolino, V. Gandin, In vitro and in vivo anticancer activity of tridentate thiosemicarbazone copper complexes: unravelling an unexplored pharmacological target, Eur. J. Med. Chem. 194 (2020) 112266.
[13] Z. Liu, S. Wu, Y. Wang, R. Li, J. Wang, L. Wang, Y. Zhao, P. Gong, Design, synthesis and biological evaluation of novel thieno[3,2-d]pyrimidine derivatives possessing diaryl semicarbazone scaffolds as potent antitumor agents, Eur. J. Med. Chem. 87 (2014) 782–793.
[14] B. Sarkanj, M. Molnar, M. Cacic, L. Gille, 4-Methyl-7-hydroxycoumarin antifungal and antioxidant activity enhancement by substitution with thiosemicarbazide and thiazolidinone moieties, Food Chem. 139 (2013) 488–495.
[15] P. Padmanabhan, S. Khaleefathullah, K. Kaveri, G. Palani, G. Ramanathan, S. Thennarasu, U. Tirichurapalli Sivagnanam, Antiviral activity of thiosemicarbazones derived from alpha-amino acids against dengue virus, J. Med. Virol. 89 (2017) 546–552.
[16] P. Chellan, N. Shunmoogam-Gounden, D.T. Hendricks, J. Gut, P.J. Rosenthal, C. Lategan, P.J. Smith, K. Chibale, G.S. Smith, Synthesis, structure and in vitro biological screening of palladium(II) complexes of functionalised salicylaldimine thiosemicarbazones as antimalarial and anticancer agents, Eur J Inorg Chem, 2010 (2010) 3520–3528.
[17] M.G. Temraz, P.A. Elzahhar, A.B.A. El-Din, A.A. Bekhit, H.F. Labib, A.S.F. Belal, Anti-leishmanial click modifiable thiosemicarbazones: design, synthesis, biological evaluation and in silico studies, Eur. J. Med. Chem. 151 (2018) 585–600.
[18] J.L. de Melos, E.C. Torres-Santos, S. Faioes Vdos, N. Del Cistia Cde, C.M. Sant'Anna, C.E. Rodrigues-Santos, A. Echevarria, Novel 3,4-methylenedioxyde-6-X-benzaldehyde-thiosemicarbazones: synthesis and antileishmanial effects against Leishmania amazonensis, Eur. J. Med. Chem. 103 (2015) 409–417.
[19] M.D. Hall, K.R. Brimacombe, M.S. Varonka, K.M. Pluchino, J.K. Monda, J. Li, M.J. Walsh, M.B. Boxer, T.H. Warren, H.M. Fales, M.M. Gottesman, Synthesis and structure-activity evaluation of isatin-beta-thiosemicarbazones with improved selective activity toward multidrug-resistant cells expressing P-glycoprotein, J. Med. Chem. 54 (2011) 5878–5889.
[20] M.L. Pati, M. Niso, D. Spitzer, F. Berardi, M. Contino, C. Riganti, W.G. Hawkins, C. Abate, Multifunctional thiosemicarbazones and deconstructed analogues as a strategy to study the involvement of metal chelation, Sigma-2 (sigma 2) receptor and P-gp protein in the cytotoxic action: in vitro and in vivo activity in pancreatic tumors, Eur. J. Med. Chem. 144 (2018) 359–371.
[21] J.F. de Oliveira, T.S. Lima, D.B. Vendramini-Costa, S.C.B. de Lacerda Pedrosa, E.A. Lafayette, R.M.F. da Silva, S.M.V. de Almeida, R.O. de Moura, A. Ruiz, J.E. de Carvalho, M. de Lima, Thiosemicarbazones and 4-thiazolidinones indole-based derivatives: synthesis, evaluation of antiproliferative activity, cell death mechanisms and topoisomerase inhibition assay, Eur. J. Med. Chem. 136 (2017) 305–314.
[22] F. Vandresen, H. Falzirolli, S.A. Almeida Batista, A.P. da Silva-Giardini, D.N. de Oliveira, R.R. Catharino, A.L. Ruiz, J.E. de Carvalho, M.A. Foglio, C.C. da Silva, Novel R-(+)-limonene-based thiosemicarbazones and their antitumor activity against human tumor cell lines, Eur. J. Med. Chem. 79 (2014) 110–116.
[23] P.C.S. Danuta, S. Kalinowski, Paul V. Bernhardt, Des R. Richardson, Design, synthesis, and characterization of new iron chelators with anti-proliferative activity: structure-activity relationships of novel thiohydrazone analogues, J. Med. Chem. 50 (2007) 6212–6225.
[24] Y. Yu, D.S. Kalinowski, Z. Kovacevic, A.R. Siafakas, P.J. Jansson, C. Stefani, D.B. Lovejoy, P.C. Sharpe, P.V. Bernhardt, D.R. Richardson, Thiosemicarbazones from the old to new: iron chelators that are more than just ribonucleotide reductase inhibitors, J. Med. Chem. 52 (2009) 5271–5294.
[25] B.M. Zeglis, V. Divilov, J.S. Lewis, Role of metalation in the topoisomerase IIalpha inhibition and antiproliferation activity of a series of alpha-heterocyclic-N4-substituted thiosemicarbazones and their Cu(II) complexes, J. Med. Chem. 54 (2011) 2391–2398.
[26] D.B. Lovejoy, D.M. Sharp, N. Seebacher, P. Obeidy, T. Prichard, C. Stefani, M.T. Basha, P.C. Sharpe, P.J. Jansson, D.S. Kalinowski, P.V. Bernhardt, D.R. Richardson, Novel second-generation di-2-pyridylketone thiosemicarbazones show synergism with standard chemotherapeutics and demonstrate potent activity against lung cancer xenografts after oral and intravenous administration in vivo, J. Med. Chem. 55 (2012) 7230–7244.
[27] P.C.S. Des R. Richardson, David B. Lovejoy, Dakshita Senaratne, Danuta S. Kalinowski, Mohammad Islam, Paul V. Bernhardt, Dipyridyl thiosemicarbazone chelators with potent and selective antitumor activity form iron complexes with redox activity, J. Med. Chem. 49 (2006) 6510–6521.
[28] M.S.L. Zhi-Gang Jiang, Hossein A. Ghanbari, Neuroprotective activity of 3-aminopyridine-2-carboxaldehyde thiosemicarbazone (PAN-811), a cancer therapeutic agent, CNS Drug Rev. 12 (2006) 77–90.
[29] H.E. Elsayed, H.Y. Ebrahim, E.G. Haggag, A.M. Kamal, K.A. El Sayed, Rationally designed hecogenin thiosemicarbazone analogs as novel MEK inhibitors for the control of breast malignancies, Bioorg. Med. Chem. 25 (2017) 6297–6312.
[30] C. Guo, L. Wang, X. Li, S. Wang, X. Yu, K. Xu, Y. Zhao, J. Luo, X. Li, B. Jiang, D. Shi, Discovery of novel bromophenol-thiosemicarbazone hybrids as potent selective inhibitors of poly(ADP-ribose) polymerase-1 (PARP-1) for use in cancer, J. Med. Chem. 62 (2019) 3051–3067.
[31] S.Y. Abbas, R.A.K. Al-Harbi, M.A.M. Sh El-Sharief, Synthesis and anticancer activity of thiourea derivatives bearing a benzodioxole moiety with EGFR inhibitory activity, apoptosis assay and molecular docking study, Eur. J. Med. Chem. 198 (2020) 112363.
[32] A.G. Ribeiro, S.M.V.d. Almeida, J.F. de Oliveira, T.R.C.d.L. Souza, K.L.d. Santos, A.P.d.B. Albuquerque, Novel 4-quinoline-thiosemicarbazone derivatives: synthesis, antiproliferative activity, in vitro and in silico biomacromolecule interaction studies and topoisomerase inhibition, Eur. J. Med. Chem. 182 (2019) 111592.
[33] A. Lindemann, A.A. Patel, N.L. Silver, L. Tang, Z. Liu, L. Wang, N. Tanaka, X. Rao, H. Takahashi, N.K. Maduka, M. Zhao, T.C. Chen, W. Liu, M. Gao, J. Wang, S.J. Frank, W.N. Hittelman, G.B. Mills, J.N. Myers, A.A. Osman, COTI-2, a novel thiosemicarbazone derivative, exhibits antitumor activity in HNSCC through p53-dependent and -independent mechanisms, Clin. Canc. Res. 25 (2019) 5650–5662.
[34] K.M. Anna Mrozek-Wilczkiewicz, Marta Rejmund, Jaroslaw Polanski, Robert Musiol Anticancer activity of the thiosemicarbazones that are based on di-2 pyridine ketone and quinoline moiety, Eur. J. Med. Chem. 171 (2019) 180–194.
[35] J.F. de Oliveira, A.L. da Silva, D.B. Vendramini-Costa, C.A. da Cruz Amorim, J.F. Campos, A.G. Ribeiro, R. Olimpio de Moura, J.L. Neves, A.L. Ruiz, J. Ernesto de Carvalho, C. Alves de Lima Mdo, Synthesis of thiophene-thiosemicarbazone derivatives and evaluation of their in vitro and in vivo antitumor activities, Eur. J. Med. Chem. 104 (2015) 148–156.
[36] L.Y. Ma, Y.C. Zheng, S.Q. Wang, B. Wang, Z.R. Wang, L.P. Pang, M. Zhang, J.W. Wang, Design, synthesis, and structure-activity relationship of novel LSD1 inhibitors based on pyrimidine-thiourea hybrids as potent, orally active antitumor agents, J. Med. Chem. 58 (2015) 1705–1716.
[37] B. Hu, B. Wang, B. Zhao, Q. Guo, Z.H. Li, X.H. Zhang, G.Y. Liu, Y. Liu, Y. Tang, F. Luo, Y. Du, Y.X. Chen, L.Y. Ma, H.M. Liu, Thiosemicarbazone-based selective proliferation inactivators inhibit gastric cancer cell growth, invasion, and migration, Medchemcomm 8 (2017) 2173–2180.
[38] X.H. Zhang, W. Bo, Y.Y. Tao, Q. Ma, H.J. Wang, Z.X. He, H.P. Wu, Y.H. Li, B. Zhao, L.Y. Ma, H.M. Liu, Thiosemicarbazone-based lead optimization to discover high-efficiency and low-toxicity anti-gastric cancer agents, Eur. J. Med. Chem. 199 (2020) 112349.
[39] Z. He, H. Qiao, F. Yang, W. Zhou, Y. Gong, X. Zhang, H. Wang, B. Zhao, L. Ma, H.M. Liu, W. Zhao, Novel thiosemicarbazone derivatives containing indole fragment as potent and selective anticancer agent, Eur. J. Med. Chem. 184 (2019) 111764.
[40] S. Dadashpour, S. Emami, Indole in the target-based design of anticancer agents: a versatile scaffold with diverse mechanisms, Eur. J. Med. Chem. 150 (2018) 9–29.
[41] J.A. Bergman, K. Woan, P. Perez-Villarroel, A. Villagra, E.M. Sotomayor, A.P. Kozikowski, Selective histone deacetylase 6 inhibitors bearing substituted urea linkers inhibit melanoma cell growth, J. Med. Chem. 55 (2012), 9891-8999.
[42] P. Chellan, N. Shunmoogam-Gounden, D.T. Hendricks, J. Gut, P.J. Rosenthal, C. Lategan, P.J. Smith, K. Chibale, G.S. Smith, Synthesis, structure and in vitro biological screening of palladium(II) complexes of functionalised salicylaldimine thiosemicarbazones as antimalarial and anticancer agents, Eur J Inorg Chem, 2010 (2010) 3520–3528.
[43] D.R.R. Danuta S. Kalinowski, Future of toxicologyslron chelators and differing modes of action and toxicity: the changing face of iron chelation therapy, Chem. Res. Toxicol. 20 (2007) 716–720.
[44] K. Engeland, Cell cycle arrest through indirect transcriptional repression by p53: I have a dream, Cell Death Differ. 25 (2017) 114–132.
[45] C.F. Lee, J.S. Yang, F.J. Tsai, N.N. Chiang, C.C. Lu, Y.S. Huang, C. Chen, F.A. Chen, Kaempferol induces ATM/p53-mediated death receptor and mitochondrial

apoptosis in human umbilical vein endothelial cells, Int. J. Oncol. 48 (2016) 2007–2014.
[46] J.N. Moloney, T.G. Cotter, ROS signalling in the biology of cancer, Semin. Cell Dev. Biol. 80 (2018) 50–64.
[47] Y. Liu, D. Fan, Ginsenoside Rg5 induces G2/M phase arrest, apoptosis and autophagy via regulating ROS-mediated MAPK pathways against human gastric cancer, Biochem. Pharmacol. 168 (2019) 285–304.
[48] J. Yang, S. Hu, C. Wang, J. Song, C. Chen, Y. Fan, Y. Ben-David, W. Pan, Fangchinoline derivatives induce cell cycle arrest and apoptosis in human leukemia cell lines via suppression of the PI3K/AKT and MAPK signaling pathway, Eur. J. Med. Chem. 186 (2019) 111898.
[49] J.D. Cohen, K.Y. Tham, N.J. Mastrandrea, A.C. Gallegos, T.J. Monks, S.S. Lau, cAMP-dependent cytosolic mislocalization of p27(kip)-cyclin D1 during quinol-thioether-induced tuberous sclerosis renal cell carcinoma, Toxicol. Sci. 122 (2011) 361–371.